



crystals



Review

From Processing to Performance: Innovations and Challenges in Ceramic-Based Materials

Sachin Kumar Sharma, Sandra Gajević, Lokesh Kumar Sharma, Yogesh Sharma, Mohit Sharma, Saša Milojević, Slobodan Savić and Blaža Stojanović



<https://doi.org/10.3390/crust16020085>

Review

From Processing to Performance: Innovations and Challenges in Ceramic-Based Materials

Sachin Kumar Sharma ^{1,*}, Sandra Gajević ^{2,*}, Lokesh Kumar Sharma ³, Yogesh Sharma ⁴, Mohit Sharma ⁵, Saša Milojević ^{2,*}, Slobodan Savić ² and Blaža Stojanović ²

¹ Surface Science and Tribology Lab, Department of Mechanical Engineering, Shiv Nadar Institution of Eminence, Gautam Buddha Nagar, Greater Noida 201314, India

² Faculty of Engineering, University of Kragujevac, Sestre Janjić 6, 34000 Kragujevac, Serbia; ssavic@kg.ac.rs (S.S.); blaza@kg.ac.rs (B.S.)

³ Department of Physics, GLA University, Mathura 281406, India; lokesh.sharma@glau.ac.in

⁴ Department of Physics & Environmental Sciences, Sharda School of Engineering & Science, Sharda University, Greater Noida 201310, India; uvsbhu@gmail.com

⁵ Department of Physics and Material Science, Jaypee University, Anoopshahr 203390, India; mohit.sharma@mail.jaypeeu.ac.in

* Correspondence: ss393@snu.edu.in (S.K.S.); sandrav@kg.ac.rs (S.G.); sasa.milojevic@kg.ac.rs (S.M.)

Abstract

In aerospace, defense, and energy systems, ceramic matrix composites (CMCs) are smart structural materials designed to function continuously in harsh mechanical, thermal, and oxidative conditions. Using high-strength fiber reinforcements and tailored interphases that enable damage-tolerant behavior, their creation tackles the intrinsic brittleness and low fracture toughness of monolithic ceramics. With a focus on chemical vapor infiltration, polymer infiltration and pyrolysis, melt infiltration, and additive manufacturing, this paper critically analyzes current developments in microstructural design, processing technologies, and interfacial engineering. Toughening mechanisms are examined in connection to multiscale mechanical responses, including controlled debonding, fiber bridging, fracture deflection, and energy dissipation pathways. Cutting-edge environmental barrier coatings are assessed alongside environmental durability issues like oxidation, volatilization, and hot corrosion. High-performance braking, nuclear systems, hypersonic vehicles, and turbine propulsion are evaluated as emerging uses. Future directions emphasize self-healing systems, ultra-high-temperature design, and environmentally friendly production methods.

Keywords: ceramic matrix composites (CMCs); high-temperature structural ceramics; extrinsic toughening mechanisms; ultra-high temperature ceramics (UHTCs); aerospace and propulsion systems



Academic Editors: Daisuke Nakauchi and Vladislav V. Kharton

Received: 28 December 2025

Revised: 21 January 2026

Accepted: 23 January 2026

Published: 25 January 2026

Copyright: © 2026 by the authors.

Licensee MDPI, Basel, Switzerland. This article is an open access article distributed under the terms and conditions of the [Creative Commons Attribution \(CC BY\) license](https://creativecommons.org/licenses/by/4.0/).

1. Introduction

Advanced structural materials such as ceramic matrix composites (CMCs) are increasingly required where conventional metallic alloys and monolithic ceramics cannot withstand sustained extremes. Modern aerospace propulsion systems, hypersonic vehicles, re-entry platforms, and advanced nuclear reactors operate under high heat flux, oxidizing/corrosive environments, and cyclic thermomechanical loading [1]. Although ceramics such as silicon carbide (SiC) and alumina (Al_2O_3) offer high compressive strength and thermal stability, their brittleness, low fracture toughness, and poor flaw tolerance make them vulnerable to catastrophic failure under impact, fatigue, and thermal shock, limiting

use in damage-critical components [2]. This mismatch between intrinsic performance and damage tolerance has driven the development of CMCs.

CMCs mitigate brittle fracture by embedding continuous ceramic fibers within a ceramic matrix to enable progressive, damage-tolerant failure. Early work in the 1970s and 1980s addressed unstable crack propagation, a dominant failure mode in monolithic ceramics [3,4]. Continuous reinforcements (SiC, C, and oxide fibers) activate extrinsic toughening through crack deflection, interfacial debonding, frictional sliding, fiber bridging, and fiber pull-out, which redistribute stress and promote stable crack growth under mechanical and thermal loading [5]. Damage tolerance is therefore governed not only by fiber selection but also by microstructural design, particularly interphase architecture and processing-induced defects.

Over the past three decades, progress in microstructural design, processing, and environmental protection has enabled CMCs to transition from laboratory materials to qualified systems in certified components. Relative to Ni-based superalloys, SiC/SiC CMCs implemented in hot-section turbine hardware have enabled ~30–40% weight reduction and >10% fuel-efficiency improvement, largely due to low density and elevated-temperature mechanical retention [6]. Carbon/carbon (C/C) composites also show proven reliability in aerospace thermal protection systems (TPS) and high-energy braking, where thermal-shock resistance is essential.

Across CMC systems, performance is microstructure-controlled, with the fiber/matrix interphase as a central design lever [7]. Engineered interphases such as pyrolytic carbon (PyC) and boron nitride (BN) create compliant and chemically tuned interfaces that support crack deflection and interfacial sliding, delay fiber rupture, and improve damage tolerance [8]. Structural response also depends strongly on reinforcement architecture. Two-dimensional woven, braided, and 3D topologies govern load transfer, crack localization, porosity distribution, and thermo-mechanical fatigue resistance. As a result, CMC performance must be interpreted as architecture-dependent rather than a single intrinsic property [9].

Manufacturability has advanced through improved densification routes, including chemical vapor infiltration (CVI), polymer infiltration and pyrolysis (PIP), melt infiltration (MI), and emerging additive manufacturing (AM). These approaches enable porosity control, near-net-shape fabrication, and process flexibility for complex geometries [10]. However, production remains cost-intensive due to long cycle times, high energy demand, and strict quality requirements. Hybrid densification strategies and digitally enabled manufacturing, including automation, real-time monitoring, and reproducibility control, are therefore increasingly pursued to reduce cost and improve component consistency [11].

Despite progress, environmental durability remains a major constraint for high-temperature deployment. Fibers, interphases, and matrices degrade through active oxidation, volatilization-driven recession, and corrosion in oxidizing, steam-rich, and combustion-derived atmospheres [10–12]. Severe degradation can also result from molten-metal interaction, such as molten Al attack, corrosive ingress, and reaction-layer growth, which disrupt interphase integrity and suppress interfacial sliding [12]. Consequently, environmental barrier coatings (EBCs) are indispensable for SiC-based CMCs above ~1300–1500 °C [13]. Current EBC concepts emphasize diffusion-limiting architectures and engineered interlayers to suppress reactive transport and stabilize interfaces under coupled thermo-chemical loading [13,14]. Nevertheless, microcracking, spallation, and interfacial degradation remain persistent failure routes during long-term cycling, motivating more robust and damage-tolerant coating designs [13]. Oxide/ceramic heterostructures engineered for improved chemical stability further offer pathways to extend EBC lifetime under aggressive service [14].

Beyond SiC/SiC and oxide systems, ultra-high-temperature ceramic (UHTC) matrix composites reinforced with transition-metal carbides and borides such as ZrB₂ and HfC are promising for hypersonic and high-temperature nuclear applications [15]. However, oxidation susceptibility, processing complexity, and scalability limitations remain key barriers. At the technology level, rising demands for energy efficiency and sustainable transport further increase interest in lightweight CMCs that reduce fuel consumption and extend component lifetime [15,16]. The design space is also expanding toward multifunctional architectures, including self-healing CMCs and self-monitoring composites integrating distributed sensing [16,17]. Industrial adoption remains limited by the lack of standardized qualification pathways, insufficient predictive modeling, repair and manufacturing challenges at scale, and incomplete understanding of coupled multiscale damage evolution under thermo-chemo-mechanical loading [18]. High costs associated with high-purity fibers, precision densification routes, and complex coating architectures continue to drive innovation in materials sourcing, process efficiency, and lifecycle cost reduction [19]. This review summarizes recent progress in the science and engineering of CMCs, focusing on extrinsic toughening, processing–microstructure–property linkages, and enabling technologies for extreme-temperature service. It synthesizes key structure–property relationships governing damage tolerance and highlights emerging implementation in automotive braking, nuclear energy, aerospace propulsion, and hypersonic systems. Future research needs are identified in environmental durability, scalable manufacturing, and next-generation multifunctional and UHTC-based CMC architectures.

2. Fundamentals of Ceramic Matrix Composites

Monolithic ceramics offer high stiffness and strong high-temperature capability, yet their structural use is limited by brittleness, low fracture toughness, and poor damage tolerance. Under tensile loading or impact, cracks initiate at inherent flaws and propagate rapidly, resulting in catastrophic failure with little warning. Ceramic matrix composites (CMCs) were developed to overcome this limitation by embedding reinforcement architectures within a ceramic matrix to enable stress redistribution, progressive energy dissipation, and pseudo-ductile fracture behavior [20]. Unlike monolithic ceramics, where failure is often dominated by a single unstable fracture event, CMCs are designed for distributed and stable damage evolution, improving reliability under combined thermo-mechanical loading [21]. These attributes support demanding use in gas-turbine propulsion, hypersonic systems, re-entry structures, and advanced energy-conversion platforms, where high specific strength, creep resistance, and phase stability are essential [22].

CMCs are commonly classified by matrix chemistry, reinforcement morphology, and architectural topology. Matrix selection governs environmental durability, reinforcement compatibility, and high-temperature stability. Non-oxide matrices, mainly C and SiC, dominate extreme-temperature propulsion due to high thermal stability and creep resistance, along with compatibility with low-density high-strength fibers [23]. However, these systems typically require environmental protection because they remain vulnerable to active oxidation, recession, and corrosion in steam-rich and combustion-derived environments. Oxide matrices such as mullite and Al₂O₃ provide improved chemical inertness and intrinsic oxidation resistance, but their high-temperature mechanical retention and thermal-shock tolerance are often lower, particularly under steep thermal gradients [24]. Ultra-high-temperature ceramic (UHTC) matrices based on Zr/Hf carbides and borides are increasingly considered for hypersonic leading edges and nuclear materials above ~2000–3000 °C. Their structural deployment remains limited by rapid oxidation in realistic atmospheres, processing complexity, and grain-growth control [20–24].

The reinforcing phase largely determines load-bearing capacity and toughness retention. For safety-critical components, continuous ceramic fibers are preferred because they enable crack arrest and sustain energy dissipation over large volumes [25]. Polycrystalline SiC fibers offer improved stability and creep resistance above \sim 1400–1600 °C, making SiC/SiC CMCs a benchmark for commercial turbine hardware [26]. Carbon fibers provide excellent stability in inert environments and remain essential in C/C composites for thermal protection and high-energy braking [27]. Oxide fibers maintain chemical stability in oxidizing atmospheres, but long-term high-load performance can be limited by grain-boundary sliding and diffusional creep, depending on fiber chemistry and processing [26–28]. Discontinuous reinforcements such as whiskers and particles have been studied as lower-cost options, yet limited load transfer and restricted strain tolerance reduce reliability under cyclic service, limiting their use in structural-grade CMCs [29]. Reinforcement selection must therefore align with processing route and operating environment, since fiber degradation and interphase stability directly control toughening retention.

Macroscopic behavior is governed by multiscale architecture, ranging from anisotropic unidirectional (UD) layups to 2D woven and 3D woven/braided/stitched forms [30]. Advances in textile engineering and digitally controlled manufacturing have enabled spatially graded architectures matched to non-uniform stress fields, which is valuable in impact- and vibration-prone environments [29,30]. Architecture affects not only strength but also damage localization, delamination resistance, and out-of-plane performance, shaping component-level damage tolerance [30].

A key differentiator of CMCs is the engineered fiber/matrix interphase, which serves as both a mechanical transition region and a chemical buffer. By controlling interfacial shear stress, the interphase enables debonding, crack deflection, sliding, fiber bridging, and pull-out, thereby converting brittle fracture into stable damage evolution [31]. Pyrolytic carbon (PyC) interphases provide high compliance and effective sliding but oxidize readily, whereas boron nitride (BN) interphases offer improved oxidation resistance but may degrade by hydrolysis in humid conditions [32]. Multilayer and graded designs such as BN/SiC and PyC/SiC are therefore used to balance mechanical response and environmental stability [33]. Interphase thickness is highly sensitive. Strong bonding suppresses sliding and promotes brittle failure, while weak bonding reduces load transfer and stiffness. In many systems, \sim 0.2–1.0 μ m provides a practical window for maximizing extrinsic toughening with limited strength penalty [34]. Reported optima vary with processing-induced porosity and residual stresses, so interphase design windows must be interpreted in the context of the manufacturing route and defect populations [31–34].

Damage evolution in CMCs proceeds through coupled mechanisms. Matrix microcracks initiate at intrinsic flaws but are deflected at the interphase, promoting crack branching and interfacial sliding [33,34]. Continued loading activates bridging and progressive pull-out, enabling inelastic strain accommodation and gradual stress redistribution, delaying collapse after matrix cracking begins [35]. These mechanisms underpin high fracture toughness, thermal-shock resistance, and fatigue endurance but depend on the coupled control of porosity, residual stress, architecture, and interphase stability. To support subsequent process–microstructure analysis, the major design variables and their roles are summarized in Table 1, highlighting that CMC performance results from interacting design choices rather than a single material selection.

Table 1. Key CMC design variables, representative options, functional roles, and major vulnerabilities.

Design Variable	Representative	Primary Role in Performance	Major Trade-Off/Vulnerability
Matrix system [15]	Non-oxide: SiC, C; Oxide: Al_2O_3 , mullite; UHTC: ZrB_2 , HfC, HfB ₂	High-T capability, chemical compatibility, stiffness, environmental durability	Non-oxide: requires EBCs; oxidation/recession in steam/combustion. Oxide: reduced high-T strength/creep resistance. UHTC: oxidation sensitivity + processing scalability barriers
Reinforcement [36]	Continuous fibers (SiC, C, oxide); discontinuous whiskers/particles	Load transfer, crack bridging, toughness retention, fatigue resistance	Fiber creep/strength degradation at high T; oxidation/hydrolysis sensitivity (system-dependent). Discontinuous reinforcements: limited strain tolerance and cyclic reliability
Architecture [37]	UD, 2D woven, braided, 3D woven/stitched	Controls anisotropy, delamination resistance, out-of-plane strength, damage containment	Higher textile complexity increases cost and defect risk (misalignment, voids, resin/infiltration non-uniformity)
Interphase [38]	PyC, BN, multilayer (BN/SiC, PyC/SiC)	Enables controlled debonding/sliding; activates extrinsic toughening mechanisms	PyC oxidation; BN hydrolysis/moisture sensitivity; thickness/continuity control is critical for balancing sliding vs. load transfer
Defect state [39]	Residual porosity, microcracks, infiltration gradients	Govern crack initiation, permeability, fatigue life, environmental ingress	High porosity lowers strength/modulus; connected pores accelerate oxidation/corrosion and coating failure

Table 1 summarizes the key CMC design variables that collectively govern damage tolerance and long-term durability. It highlights that performance is controlled not only by material selection (matrix and fibers) but also by architecture, interphase design, and processing-driven defect populations. Non-oxide matrices and advanced interphases enable high-temperature capability and extrinsic toughening yet require protection against oxidation and moisture-driven degradation. The table also shows that porosity, microcracks, and infiltration non-uniformity remain critical vulnerabilities because they reduce strength and accelerate environmental ingress, making defect control central to reliable CMC deployment [36–39].

Structure–property relationships in CMCs are further governed by fiber volume fraction, residual porosity, thermal-mismatch residual stresses, and fiber orientation distribution. Excess porosity lowers strength, increases permeability, and accelerates durability loss. In contrast, controlled micro-porosity can increase energy dissipation by promoting crack deflection and enlarging fracture surface area [40]. Residual stress also has dual effects. When properly managed, mismatch stresses assist interfacial debonding and stabilize toughening, whereas excessive stress can induce microcracking or fiber damage during processing and thermal cycling [41]. Environmental durability remains a dominant limitation, particularly for non-oxide CMCs in combustion-derived atmospheres. Therefore, environmental barrier coatings (EBCs) are essential for protecting SiC/SiC and C/C systems against oxidation, volatilization, and corrosive attack [42]. Environment–microstructure coupling is critical because oxidation-driven interphase stiffening can suppress interfacial

sliding and fiber pull-out, reducing toughening retention even when the bulk composite appears mechanically intact. This issue is discussed further in Section 6.

With these fundamentals established, CMCs are increasingly transitioning from laboratory-scale materials to qualified, field-deployed components. Relative to Ni-based superalloys, turbine-engine integration has enabled substantial weight reduction, reported up to ~40–60%, and fuel-efficiency improvements of ~10% by supporting higher operating temperatures and reduced cooling-air demand [43]. Deployment is also expanding across advanced nuclear reactors, high-performance automotive systems, and hypersonic platforms, where high specific strength and thermal efficiency are required [44]. Nevertheless, industrial scale-up remains constrained by high manufacturing costs, complex densification routes, and stringent certification requirements. Continued progress in standardized qualification frameworks, scalable densification technologies, and automation-enabled textile processing is improving reproducibility and accelerating adoption [40–44].

3. Processing and Fabrication Techniques

The selected processing route for CMCs directly determines the final microstructure, including matrix continuity, pore morphology and connectivity, residual stress distribution, and interfacial chemistry [13]. These features ultimately control thermo-mechanical reliability in extreme service environments. Unlike monolithic ceramics, CMCs must be manufactured to achieve three requirements simultaneously. The process must preserve fiber integrity, maintain interphase functionality needed for crack deflection and frictional sliding, and densify the matrix without embrittling interfaces or degrading reinforcement [28]. The key challenge is therefore not simply maximizing density but producing the correct damage-tolerant microstructure. This requires a continuous load-bearing matrix combined with a compliant, chemically stable interphase that supports extrinsic toughening [45]. Over the past three decades, chemical vapor infiltration (CVI), polymer infiltration and pyrolysis (PIP), melt infiltration (MI), and emerging hybrid and architected manufacturing approaches enabled by additive manufacturing and digitally controlled textiles have become the most widely discussed fabrication routes [46]. Each route imposes distinct trade-offs in porosity control, geometric capability, densification kinetics, oxidation tolerance, and cost [47]. Processing selection should therefore be treated as a design decision that links manufacturing constraints to targeted conditions.

3.1. Chemical Vapor Infiltration (CVI)

Chemical vapor infiltration (CVI) is among the most established routes for producing structural-grade CMCs, particularly for aerospace hot-section components where reliability is prioritized over cost. In CVI, reactive gaseous precursors infiltrate a porous fiber preform in a controlled reactor and decompose to deposit a conformal ceramic matrix, typically SiC, C, or BN, on internal fiber and pore surfaces (Figure 1a) [48]. Processing temperatures of ~1000–1200 °C help preserve fiber tensile strength and limit interphase degradation, enabling the microstructural conditions required for crack deflection and interfacial sliding. Consequently, CVI-derived SiC/SiC systems show strong high-temperature stability and relatively uniform matrix distribution [49]. Controlled residual porosity can further promote crack tortuosity and distributed microcracking, supporting energy dissipation and damage tolerance. However, densification is diffusion-limited, and achieving adequate density can require cycles lasting weeks, which increases cost and limits throughput. Residual porosity of ~10–15% often persists, reducing transverse properties and creating connected pathways for environmental ingress, which may require seal coats or secondary densification [50]. These trade-offs explain why CVI remains a performance benchmark,

while hybrid densification is increasingly adopted when cycle time, cost, or permeability becomes limiting.

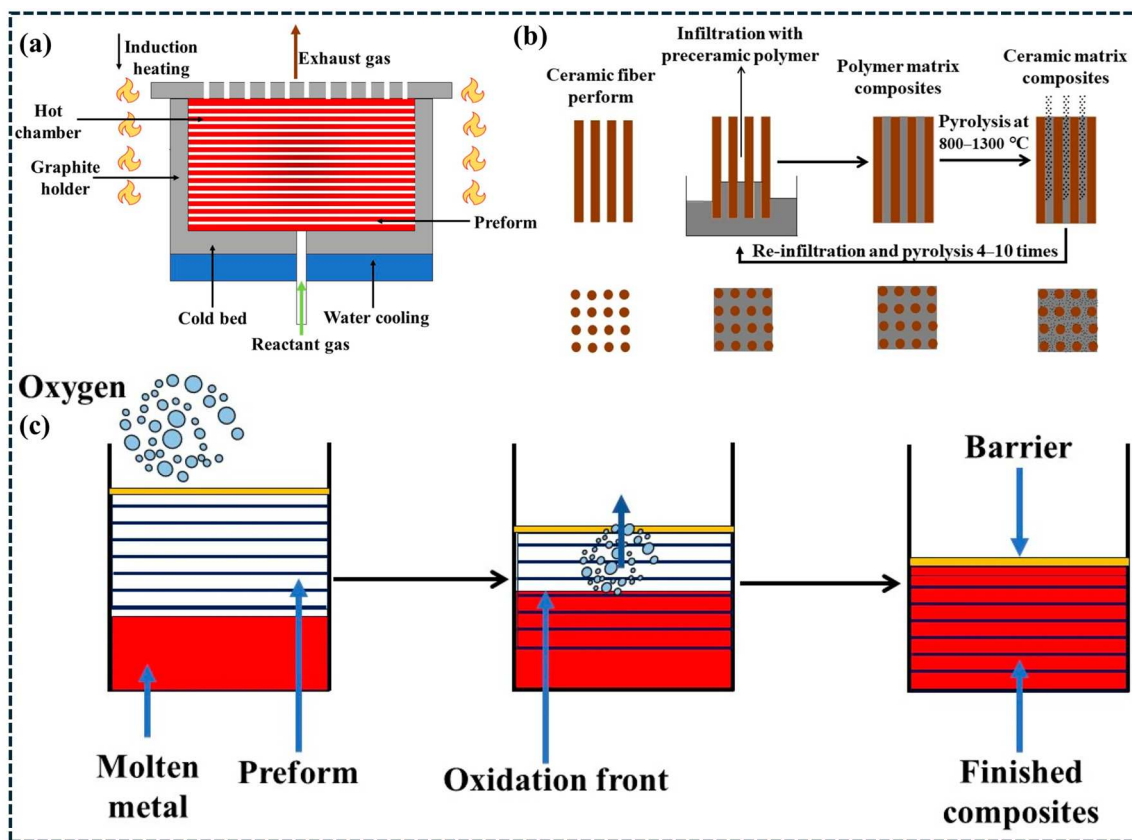


Figure 1. Schematic illustration of key CMC densification routes: (a) chemical vapor infiltration (CVI) of a porous fiber preform in a hot-wall reactor, (b) polymer infiltration and pyrolysis (PIP) showing repeated infiltration–pyrolysis cycles ($\approx 4\text{--}10$) to progressively reduce porosity, and (c) melt infiltration (MI) depicting molten metal infiltration into the preform with an advancing reaction/oxidation front leading to a dense composite [51].

3.2. Polymer Infiltration and Pyrolysis (PIP)

Polymer infiltration and pyrolysis (PIP) is a scalable and cost-effective densification route for both oxide and non-oxide CMCs, particularly suitable for complex geometries that can be infiltrated without high-cost vapor infiltration reactor infrastructure. In this approach, liquid preceramic polymers (e.g., polycarbosilane or polysilazane) infiltrate porous fiber preforms and are subsequently converted into ceramic matrices through controlled pyrolysis at relatively moderate temperatures ($\sim 800\text{--}1000\text{ }^{\circ}\text{C}$), which helps limit fiber strength degradation and preserve interphase stability (Figure 1b) [51,52]. Because the polymer-to-ceramic transformation is accompanied by substantial mass loss and volumetric shrinkage, matrix formation is inherently defect-prone and generates secondary porosity and microcracking; therefore, densification proceeds in a cycle-dependent manner and requires repeated infiltration–pyrolysis iterations to progressively reduce open porosity.

The cumulative effect of reinfiltration cycles on densification is quantitatively reflected in Figure 2a,b, where the composite density increases monotonically with the number of SMP-10 infiltration/pyrolysis cycles (Figure 2a) while the total porosity decreases sharply during early cycles followed by a saturation regime at higher cycle numbers (Figure 2b) [51]. This behavior is consistent with pore-network evolution: early cycles preferentially fill large, interconnected pores, whereas later cycles are constrained by pore isolation and limited precursor accessibility. As shown in Figure 2a,b, powder morphology also influ-

ences densification efficiency, with non-spherical powder producing higher final density and lower residual porosity due to improved packing and pore filling [52]. Nevertheless, even after multiple cycles, PIP-derived CMCs commonly retain \sim 15–25% residual porosity and shrinkage-induced microcracking, which reduces stiffness and strength and typically lowers thermal conductivity relative to melt-infiltrated systems. The remaining permeable pathways also accelerate oxidant ingress, promoting interphase degradation and reducing long-term retention of fiber sliding and pull-out toughening mechanisms during service [53]. Consequently, PIP is generally selected when a cost–performance compromise is required, including thermal insulation components, intermediate-temperature structural parts, and emerging automotive platforms, and it is frequently implemented in hybrid densification workflows to reduce total cycle count while meeting application-specific property targets [51–53].

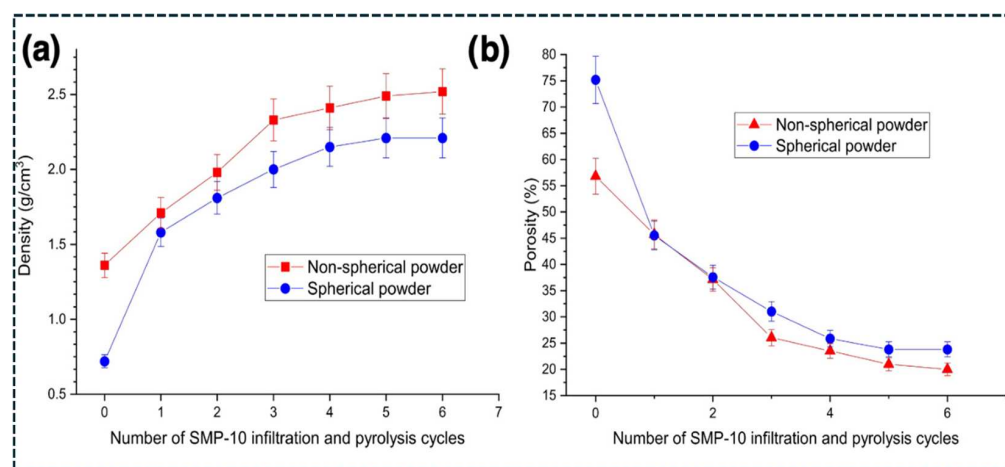


Figure 2. Evolution of densification during polymer infiltration and pyrolysis (PIP) using SMP-10 precursor: (a) bulk density and (b) porosity as a function of the number of infiltration/pyrolysis cycles for spherical and non-spherical powders, illustrating rapid porosity reduction during early cycles followed by a saturation regime at higher cycles [52].

3.3. Melt Infiltration (MI) and Hybrid Densification Strategies

Melt infiltration (MI) is attractive for rapidly producing high-density CMCs, enabling near-theoretical densification and improved thermal transport. In MI, molten precursors, most commonly Si or Si-rich alloys, infiltrate a porous preform containing C or ceramic. Reactive conversion then forms a dense ceramic matrix, such as reaction-bonded SiC (Figure 1c) [54]. The resulting low residual porosity and high thermal conductivity make MI-derived composites suitable for high heat-flux environments and steep thermal gradients. However, MI can introduce residual free Si and reaction-derived phases that reduce oxidation resistance above \sim 1250 $^{\circ}\text{C}$ and generate thermal-expansion mismatch stresses during rapid thermal transients [55]. High matrix continuity and stiffness improve load transfer and strength but can also restrict interphase sliding and reduce crack deflection if interphase response becomes constrained [54,55]. These limitations of single-route fabrication have motivated hybrid densification. In industrial workflows, CVI is often applied first to preserve fiber integrity and interphase compliance, followed by MI or PIP to close remaining porosity and increase density. This approach enables application-specific control of pore connectivity, interfacial shear response, and environmental resistance [56]. Hybridization should therefore be viewed as a microstructure-balancing strategy that preserves extrinsic toughening while improving component reliability.

3.4. Additive Manufacturing (AM) and Digitally Enabled CMC Architecture

Additive manufacturing (AM) is emerging as an enabling platform for architected CMC components by expanding geometric freedom and supporting digitally integrated manufacturing. Routes such as direct ink writing (DIW), binder jetting, stereolithography (SLA/DLP), and selective laser processing have been adapted for ceramic composites using ceramic-loaded inks, preceramic polymer feedstocks, and multimodal powders [57]. The primary advantage of AM is architectural control, enabling topology-optimized designs, embedded cooling channels, graded porosity, and functionally graded geometries with reduced tooling and faster design iteration. Printed parts are typically porous green bodies, so debinding and pyrolysis are required, followed by post-densification using CVI, PIP, or MI to restore matrix continuity and recover high-temperature strength [58]. Reliability is governed by printing resolution, green density, and defect statistics, with feature sizes of $\sim 20\text{--}100\ \mu\text{m}$ for SLA/DLP and $\sim 50\text{--}300\ \mu\text{m}$ for DIW and binder jetting [59]. Post-print thermal processing commonly includes binder removal at $\sim 300\text{--}600\ ^\circ\text{C}$ under controlled heating, followed by stabilization or pyrolysis of the scaffold [60].

Because AM-derived structures remain highly porous, structural-grade AM CMCs generally require extensive post-densification. CVI is often used to deposit a high-purity ceramic skeleton, sometimes requiring tens to hundreds of hours depending on thickness [61]. PIP is frequently applied as a sealing step through multiple cycles, commonly $\sim 5\text{--}10$, to reduce connected porosity. MI is selected when rapid densification and high thermal conductivity are required [62]. A key limitation is the defect population introduced by layerwise processing, including interlayer pores, anisotropic bonding, and shrinkage gradients. These defects can dominate strength scatter and fatigue reliability unless post-densification eliminates connected porosity and restores matrix continuity [63]. Key challenges include preserving interphase integrity during processing, minimizing heterogeneous shrinkage, enabling uniform infiltration of complex internal channels, and achieving reproducible defect statistics suitable for certification [64]. AM-enabled CMCs should therefore be treated as architecture-expanding systems whose performance ultimately depends on densification quality and robust QA (quality assurance) and NDE (non-destructive evaluation) control. Table 2 summarizes the dominant microstructural outcomes, advantages, limitations, and application domains associated with CVI, PIP, MI, and AM routes.

Table 2. Compact comparison of CMC processing routes.

Route	Residual Porosity	Main Advantages	Main Limitations	Cost/Scalability	Typical Applications
CVI [49]	$\sim 10\text{--}20\%$	High purity matrix, excellent interphase retention, strong high-T stability	Weeks-long cycles, high cost, porosity persists	Moderate scale, high cost	Aerospace hot-section SiC/SiC, combustors, shrouds, nozzles
PIP [52]	$\sim 15\text{--}30\%$	Low equipment cost, good geometry infiltration, near-net shape, hybrid-ready	Many cycles, shrinkage microcracks, lower k and strength	High scale, low-moderate cost	Cost-sensitive CMCs, TPS, mid-T structures, preforms for CVI or MI
MI [55]	$<5\text{--}10\%$	Fast densification, high k , higher strength	Free Si or phases, high-T oxidation limits, brittleness risk	High scale, moderate cost	Dense SiC-based parts, heat exchangers, high heat-flux hardware
AM + post-dens. [58]	Route-dependent	Complex shapes, channels, graded architectures, rapid iteration	Defects and anisotropy, needs densification, QA challenges	Moderate now, high potential	Architected CMCs, lattices, cooling-channel components

Table 2 compares the major CMC fabrication routes and highlights the trade-off between densification quality, defect control, and manufacturing cost. CVI provides high-purity matrices and strong interphase retention but requires long cycle times and retains residual porosity [49]. PIP offers scalable and low-cost processing, though shrinkage microcracking and higher porosity can reduce durability without hybrid densification [52]. MI enables rapid, high-density matrices with improved thermal transport, but residual phases can limit high-temperature stability and oxidation resistance [55], while AM expands architectural freedom but remains governed by post-densification quality and QA reliability [58].

3.5. Processing–Microstructure Control and Linkage to Extrinsic Toughening

Extrinsic toughening in CMCs, including crack deflection, fiber bridging, fiber pull-out, frictional sliding, and controlled interfacial debonding, is often described through reinforcement architecture and interphase chemistry. In practice, its activation and long-term retention are equally governed by the processing-defined microstructure. Processing controls residual porosity and connectivity (intra-tow vs. inter-tow), matrix continuity and stiffness distribution, interphase thickness and chemical stability, and residual thermal stresses from shrinkage and thermal expansion mismatch [59]. These factors collectively define crack initiation, crack-path tortuosity, interfacial sliding resistance, and bridging stability under cyclic thermo-mechanical loading. Therefore, toughness in CMCs is an emergent outcome of process-driven microstructure, not a single intrinsic material property. In CVI, gas-phase deposition produces high-purity matrices with minimal fiber damage and strong retention of PyC or BN interphases, which support stable crack deflection and sliding [60]. However, diffusion-limited densification often leaves ~10–20 vol.% porosity, which can become connected and accelerate environmental ingress. Oxidation-driven interphase stiffening then suppresses sliding and pull-out, reducing toughness retention [61].

In PIP, polymer shrinkage during pyrolysis introduces microcracks and higher porosity. Residual porosity typically remains ~15–30 vol.% unless many cycles are used. While microcracking can increase crack tortuosity and promote distributed damage, high permeability accelerates environmental attack and interphase degradation [62,63]. Toughening retention therefore depends strongly on oxidation protection and hybrid densification to reduce connected porosity. In MI, molten infiltration enables rapid densification and high matrix continuity, commonly achieving <5–10 vol.% porosity. This improves load transfer and increases bridging stress, while reduced permeability limits oxidant transport [64]. However, residual phases such as free Si and reaction products can create stiffness gradients and brittle behavior at elevated temperatures, requiring strict control of chemistry and interphase stability. AM expands architectural control through lattice structures, graded porosity, and integrated channels that can tailor crack paths and stress redistribution. However, layerwise processing introduces defects such as interlayer pores and anisotropic bonding, which can dominate strength scatter [65]. Structural-grade AM CMCs therefore require post-densification using CVI, PIP, or MI, and performance depends on defect elimination and robust QA. Overall, the most reliable CMCs are produced within a balanced processing window. Densification must ensure load-bearing integrity and low permeability, while interphase compliance and controlled heterogeneity must be preserved to sustain extrinsic toughening during long-term service [66]. Table 3 summarizes processing-driven microstructural signatures and their implications for toughening retention in harsh environments.

Table 3. Processing-driven microstructure and its impact on extrinsic toughening retention in CMCs.

Processing Route	Dominant Microstructural Signatures	Primary Impact on Extrinsic Toughening	Toughening Retention Under High T, Fatigue, and Oxidative Exposure
CVI [61]	Residual porosity ~10–20%, relatively uniform matrix deposition, high purity, strong interphase integrity	Promotes crack deflection and stable frictional sliding. Enables pull-out when the interphase remains protected. Residual pores increase crack tortuosity but can initiate fatigue damage if connected	Moderate to high, limited by connected porosity and environmental ingress
PIP [63]	Residual porosity ~15–30% depending on cycle count, shrinkage-induced microcracks, matrix heterogeneity	Increases crack tortuosity and distributed microcracking. Sliding and pull-out are achievable but strongly controlled by permeability and interphase oxidation resistance	Moderate, often decreases unless porosity is reduced and hybrid densification is applied
MI [64]	Low porosity < 5–10%, high matrix continuity, possible free Si and reaction phases, local stiffness gradients	Improves load transfer and increases bridging stresses. Crack deflection can be reduced if brittle phases dominate. Residual phases can shift interfacial shear response	Variable, often high initially but can decline at elevated temperature if residual phases degrade
AM + post-densification [65]	Architecture-defined features such as lattices and graded regions, defect sensitivity from interlayer pores, final microstructure governed by post-densification route	Toughening can be enhanced through designed crack-arrest and bridging zones. Performance is strongly controlled by defect elimination and post-densification quality	Currently moderate, improving with stronger process control and QA maturity

Table 3 summarizes how each processing route defines the dominant microstructural signature in CMCs and therefore controls extrinsic toughening activation and retention. It clarifies that CVI provides strong interphase preservation and stable sliding-based toughening, but toughness retention is limited when residual porosity becomes connected and enables environmental ingress [61]. PIP promotes crack tortuosity through shrinkage microcracking, yet higher porosity and permeability often accelerate interphase degradation unless hybrid densification is applied [63]. MI achieves high matrix continuity and strong load transfer with low porosity, although residual-free Si and stiffness gradients can reduce crack deflection and degrade high-temperature performance [64]. AM expands toughening through architecture-driven crack-arrest features, but retention remains governed by defect control and post-densification quality [65].

3.6. Textile Architectures, QA/NDE Integration, and Manufacturability Constraints

Beyond densification route selection, CMC performance is strongly controlled by fiber preform architecture and the manufacturability of complex reinforcement designs. Advanced textile processing enables 2D and 3D woven, braided, and stitched preforms that increase through-thickness reinforcement, improve delamination resistance, and enhance damage containment under multiaxial loading [66]. Automated fiber placement, robotic braiding, and digitally programmable weaving provide tight control of fiber orientation, spatial distribution, and fiber volume fraction, enabling localized reinforcement matched to

component-specific stress fields and vibration or impact demands [9]. However, increased architectural complexity also increases infiltration difficulty. Pore isolation, partial infiltration, and heterogeneous densification become more likely, which introduces stiffness gradients and reduces fatigue reliability [67]. Quality assurance therefore increasingly depends on in-process monitoring and non-destructive evaluation (NDE). Thermography, acoustic emission, phased-array ultrasonics, and high-resolution X-ray computed tomography are widely applied to quantify porosity gradients, detect fiber misalignment or fracture, and assess interphase continuity during manufacturing and service exposure [68]. These tools are essential for qualifying safety-critical aerospace and nuclear components where defect tolerance is limited.

3.7. Cost Drivers, Processing Environment Control, and Emerging Multifunctional Fabrication

From an industrial perspective, cost remains a primary barrier to large-scale CMC adoption. Long cycle times, expensive precursor chemistries, energy-intensive thermal processing, and stringent QA requirements make CMC manufacturing significantly more complex than processing metallic alloys or monolithic ceramics. Therefore, improvements in CVI kinetics, rapid PIP cycling, and integrated hybrid densification workflows that reduce labor demand and capital intensity are directly tied to commercial viability [69]. Much of the current manufacturing investment has been driven by propulsion programs, where replacing superalloys with CMCs delivers major fuel savings, reduced cooling-air requirements, and weight reduction. As manufacturing matures, economies of scale are expected to support broader deployment in advanced automotive platforms and energy infrastructure. Thermo-chemical environment control during processing is equally critical. Oxygen partial pressure, moisture, and trace contaminants can strongly affect interphase stability, fiber surface chemistry, and matrix stoichiometry [70]. Residual stress development during cooling must also be managed. Controlled mismatch stresses can promote interfacial debonding and crack deflection, whereas excessive mismatch can induce fabrication microcracking and accelerate fatigue damage [71]. Recent research increasingly targets integrated damage-mitigation functions within the composite microstructure, including self-healing matrices and interphases containing Si-, B-, or aluminosilicate-based reactive phases that seal microcracks and restore barrier performance during oxidation exposure [70–72]. In parallel, multifunctional CMC architectures that integrate sensing networks, conductive pathways, and tailored thermal–electrical coupling are being developed for structural health monitoring and adaptive thermal management [73]. Overall, continued advances in CMC processing science remain central to industrial expansion, with manufacturing trends increasingly focused on rapid densification, scalable automation, and improved environmental durability while preserving the damage-tolerant behavior enabled by optimized microstructures.

4. Mechanical Behavior and Performance Parameters

CMCs differ from monolithic ceramics by enabling progressive damage accumulation rather than catastrophic brittle failure. This behavior originates from hierarchical microstructures in which continuous ceramic fibers are embedded in a ceramic matrix and separated by engineered, chemically tailored interphases [74]. The interphase is an active functional layer that governs crack deflection, controlled debonding, frictional sliding, and fiber bridging, enabling distributed energy dissipation across multiple length scales. As a result, CMCs retain meaningful residual load-bearing capability under harsh environments involving oxidative atmospheres, elevated temperatures, thermo-mechanical fatigue, and steep thermal gradients [75]. This shift in failure mode has established CMCs as enabling structural materials for advanced propulsion hardware, hypersonic platforms, nuclear

technologies, and safety-critical automotive and industrial components, where conventional alloys and monolithic ceramics reach fundamental performance limits [76]. Under tensile loading, CMCs exhibit a characteristic nonlinear stress-strain response. Following an initial elastic regime, matrix microcracking initiates and accumulates rather than triggering immediate collapse. These cracks are arrested or deflected at the engineered fiber–matrix interphase, which enables controlled debonding and frictional sliding for fracture energy dissipation [77]. Load is then redistributed to the continuous fibers, allowing the composite to sustain stress after matrix cracking and producing pseudo-ductility and high damage tolerance relative to monolithic ceramics [78]. Figure 3a–c summarizes this structure–property mechanism coupling by linking the characteristic nonlinear stress–strain response of CMCs with the underlying fracture processes [77,78]. As shown schematically in Figure 3a, matrix cracking is followed by crack deflection at the engineered interphase and progressive interfacial sliding, which delays catastrophic failure and enables continued load bearing beyond the proportional limit. Representative fracture-surface micrographs (Figure 3b,c) further confirm extensive fiber pull-out and interphase debonding, demonstrating that energy dissipation is dominated by extrinsic toughening mechanisms rather than unstable brittle fracture [78]. Reported tensile strain-to-failure and fractured energy values for continuous-fiber CMCs can exceed those of monolithic ceramics by roughly an order of magnitude. However, this improvement depends strongly on interphase integrity and processing-induced defect states, particularly connected porosity, which directly links tensile reliability to the processing–microstructure framework discussed in Section 3 [79].

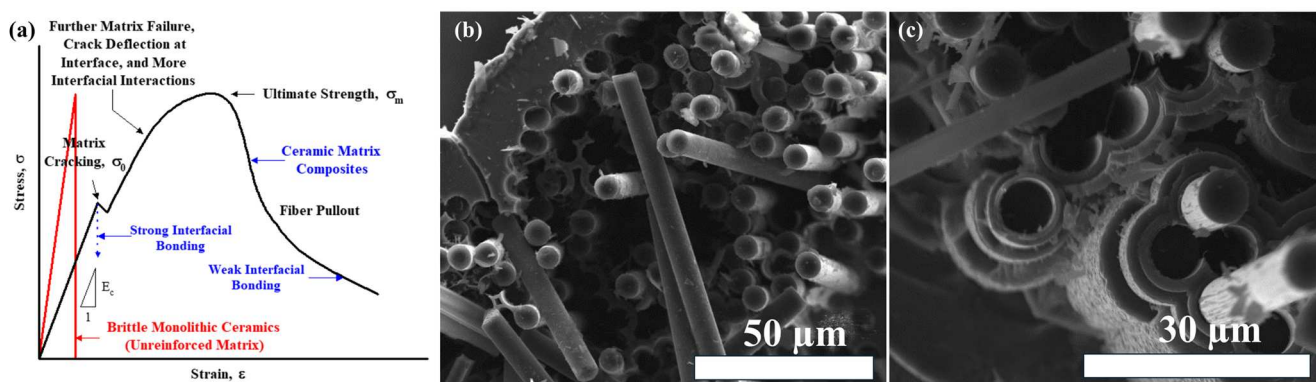


Figure 3. Mechanical response and fracture mechanisms of CMCs: (a) schematic stress–strain behavior highlighting matrix cracking, crack deflection/interfacial sliding and fiber pull-out-dominated toughening compared with brittle monolithic ceramics [77], and (b,c) representative fracture-surface SEM micrographs showing extensive fiber pull-out and interfacial debonding features that underpin damage tolerance [78].

For high-performance SiC/SiC, room-temperature tensile strengths of ~200–350 MPa and retention of ~180–300 MPa up to ~1400 °C are commonly reported, confirming suitability for elevated-temperature load-bearing applications [80]. In comparison, carbon-fiber-reinforced ceramic systems can maintain integrity in inert atmospheres up to ~2000–2200 °C but degrade rapidly in oxygen-containing environments without robust protection [81]. Oxide-based CMCs typically show tensile strengths of ~100–250 MPa, while high-temperature capability is constrained by creep and microstructural coarsening above ~1100 °C [82]. Overall, non-oxide CMCs dominate extreme-temperature deployments, but their performance advantage is realized only when interphase and coating durability are maintained under aggressive exposure. Compressive behavior in CMCs is governed by fiber buckling and micro-kinking, matrix cracking, and interfacial stability. SiC/SiC composites typically report compressive strengths of ~450–700 MPa, with wide variation

due to architecture, alignment quality, and fiber volume fraction [83]. Flexural strength, which is critical in bending-dominated applications such as turbine shrouds and thermal protection structures, commonly falls within ~ 300 – 600 MPa and remains highly sensitive to porosity and infiltration uniformity [84]. This architecture dependence directly connects Section 4 to Section 3 because densification routes that improve density can also alter pore morphology and residual stress fields, which in turn modify compressive stability and flexural reliability.

Elastic modulus values typically span ~ 150 – 420 GPa depending on fiber type and topology. Notably, SiC/SiC systems can maintain relatively stable stiffness up to ~ 1400 $^{\circ}$ C, enabling lightweight structures under extreme thermal exposure without major modulus loss [85]. This stiffness increases the importance of residual stress management and coating durability because stiffness retention alone does not guarantee retention of toughening once interphase degradation begins [86]. Fracture toughness in CMCs results from coupled extrinsic mechanisms, including crack deflection, matrix microcracking, fiber bridging, and frictional sliding [87]. Monolithic ceramics typically exhibit $K_1C \sim 3$ – 5 MPa \sqrt{m} , whereas continuous-fiber CMCs achieve much higher apparent toughness, commonly ~ 10 – 25 MPa \sqrt{m} for SiC/SiC and ~ 20 – 35 MPa \sqrt{m} for C/C systems in inert or controlled atmospheres [88]. These gains are inseparable from interphase function. Regulated debonding ahead of the crack front generates crack-closure stresses that reduce the effective stress intensity at the crack tip [89]. Post-crack fiber pull-out further increases energy absorption and stabilizes fracture. This toughening sequence is directly evidenced by the pull-out-dominated fracture morphology shown in Figure 3b,c, where long pull-out lengths and interfacial debonding traces indicate optimized interphase shear strength for controlled sliding.

Comparisons with research studies also highlight a clear design trade-off. Strong interfaces suppress sliding and promote brittle fracture, while weak interfaces reduce load transfer and stiffness [85–90]. Interphase optimization should therefore be treated as a design window rather than a single target, consistent with the processing–microstructure framework introduced in the previous Section 3.5. This is particularly important for impact-prone aerospace components that demand graceful failure modes for safety [91]. Time-dependent deformation under sustained load remains a key limitation for high-temperature deployment. Under ~ 100 – 150 MPa, SiC/SiC systems commonly show steady-state creep rates of $\sim 10^{-8}$ – 10^{-6} s $^{-1}$ at 1300 – 1400 $^{\circ}$ C, outperforming Ni-based superalloys under comparable conditions [92]. This supports use in flow-path hardware, exhaust structures, and turbine hot-section components. In contrast, oxide-based CMCs exhibit higher creep rates above ~ 1100 $^{\circ}$ C, driven by grain-boundary sliding and diffusional creep in oxide fibers, which reduces sustained-load capability [90]. Carbon-based systems show excellent intrinsic creep resistance at very high temperatures but remain unsuitable in oxidizing environments without protection, reinforcing the environment–mechanics coupling [93]. Importantly, creep is microstructure-controlled. Fiber crystallinity, fiber volume fraction, interphase stability, and matrix porosity all influence creep response, underscoring processing–microstructure–property linkage as a primary design principle.

Under cyclic mechanical and thermo-mechanical loading, CMCs exhibit progressive crack growth controlled by fiber bridging and interfacial frictional sliding. For SiC/SiC, fatigue lives of $\sim 10^5$ – 10^6 cycles at ~ 200 MPa and ~ 1100 – 1200 $^{\circ}$ C have been reported, although performance depends strongly on humidity and coating integrity [94]. Oxidation-assisted degradation of fibers and interphases in steam-rich turbine environments can reduce fatigue life by ~ 50 – 80% [90], demonstrating that fatigue is strongly coupled to environmental transport and coating durability. A practical advantage of CMCs is progressive stiffness degradation prior to failure, supporting condition-based maintenance and predictive life

management. Thermal shock resistance provides another advantage over monolithic ceramics. While monolithic ceramics often fracture during rapid transients, CMCs accommodate thermal gradients through matrix microcracking and interfacial sliding, limiting crack penetration into load-bearing fibers [95]. Tailored SiC/SiC components can tolerate quench differentials of ~ 500 – 1000 °C, depending on architecture and environmental conditions, supported by SiC's low thermal expansion coefficient of ~ 4 – 5×10^{-6} K $^{-1}$ [96]. C/C systems exhibit even higher thermal shock tolerance in inert atmospheres, consistent with their long-standing use in thermal protection structures and braking assemblies [97]. Impact response is similarly damage-tolerant. Distributed microcracking and fiber bridging localize damage and suppress fragmentation. Reported Charpy impact energies for SiC/SiC commonly lie around ~ 15 – 35 kJ m $^{-2}$, while C/C systems can exceed ~ 50 kJ m $^{-2}$, depending on porosity distribution and architecture [98]. 3D woven and braided architectures improve resistance to delamination and interlaminar shear failure relative to planar laminates, offering advantages for foreign-object-damage conditions in turbines and defense-related loading environments [99]. This reinforces the importance of architecture-optimized processing discussed in Section 3. Environmental degradation remains a dominant limiter of long-term reliability. In SiC-based CMCs, oxidation forms a protective silica scale, but under steam-rich combustion conditions the scale volatilizes, exposing fibers and interphases to accelerated recession and suppressing extrinsic toughening mechanisms [100]. Oxide-based CMCs exhibit improved oxidation stability, but mechanical performance may decline above ~ 1100 – 1200 °C due to fiber creep and grain coarsening [101]. Molten CMAS deposits can chemically attack EBC systems and trigger premature coating failure above ~ 1300 °C [102]. State-of-the-art EBC architectures have enabled reliable SiC/SiC operation beyond 1300 °C, extending lifetimes by ~ 5 – 10 times when adhesion and crack tolerance are maintained [103]. These results reinforce a central message of this review because mechanical performance in CMCs cannot be separated from environmental durability and protection strategy.

Predictive assessment increasingly relies on multiscale modeling, integrating fracture mechanics, oxidation kinetics, creep constitutive laws, and probabilistic damage accumulation [104]. These tools are being integrated into digital twin platforms for propulsion systems to enable real-time monitoring, reduce inspection burden, and extend service life beyond conservative limits [105]. Robust modeling is particularly important for certification in commercial aviation and nuclear applications, where durability under coupled mechanical and environmental loads must be demonstrated reliably [106]. Overall, CMCs provide a step change in capability relative to monolithic ceramics and many conventional alloys. Their combined elevated-temperature strength retention, enhanced fracture toughness, creep resistance, fatigue endurance, impact tolerance, and thermal shock resistance position CMCs as key materials for next-generation extreme-environment platforms [107]. To support direct comparison across material classes, Table 4 summarizes representative thermal and mechanical properties of CMCs relative to monolithic ceramics.

Table 4 summarizes representative thermal and mechanical property ranges reported for CMCs, highlighting their suitability for extreme-temperature structural applications. The table shows that SiC/SiC CMCs retain meaningful tensile strength up to 1200–1400 °C, while also offering high compressive and flexural strength with low density. It further emphasizes that superior fracture toughness and damage tolerance arise from extrinsic mechanisms such as crack deflection, fiber bridging, and pull-out [108–117]. High-temperature creep and fatigue data indicate strong durability, although performance remains sensitive to environment and microstructural condition. Overall, the table provides a compact benchmark for comparing CMC capability against monolithic ceramics and conventional alloys.

Table 4. Representative performance metrics of CMCs (primarily SiC/SiC), including strength retention, toughness, creep, fatigue, thermal shock resistance, density, and service temperature limits.

Property	CMCs (Typical Values)	Description
Tensile strength at high T (1200–1400 °C) [108]	180–300 MPa (SiC/SiC)	Tensile strength retention of SiC/SiC Mini composites under static fatigue up to 1200 °C
Compressive strength [109]	~450–700 MPa (SiC/SiC)	Strong dependence on fiber alignment and architecture
Flexural strength [110]	300–600 MPa (architecture and porosity dependent)	AM-made continuous SiC/SiC composites report flexural strength up to ~398 MPa
Apparent fracture toughness (K_1C -equivalent) [111]	10–25 MPa·m ^{1/2} (SiC/SiC)	Room-temperature fracture studies show $K_1C \sim 12$ MPa·m ^{1/2} for SiC/SiC
Damage tolerance (failure mode) [112]	Matrix microcracking with crack deflection, bridging, and pull-out	Extrinsic toughening mechanisms dominate fracture response
Creep resistance at high T [113]	10^{-8} – 10^{-6} s ⁻¹ at 1300–1400 °C (moderate stress)	Tensile creep of woven SiC/SiC composites evaluated up to 1400 °C
Fatigue life (high T cyclic loading) [114]	10^5 – 10^6 cycles at ~200 MPa, 1100–1200 °C	Oxidizing exposure reduces fatigue life due to interphase and fiber degradation
Thermal shock resistance [115]	Retains integrity under steep ΔT	Crack deflection and sliding limit through-thickness crack penetration
Density [116]	~2.5–3.2 g cm ⁻³	Low density due to fiber reinforcement and controlled porosity
Maximum service temperature [117]	1400–1600 °C (SiC/SiC) and >2000 °C (C/C in inert)	SiC/SiC for turbine hot sections, carbon systems stable in inert atmospheres

5. Toughening Mechanisms and Damage Tolerance

The fracture response of ceramic matrix composites (CMCs) differs fundamentally from that of monolithic ceramics because CMCs can sustain progressive damage accumulation rather than catastrophic brittle failure. This behavior is deliberately engineered through extrinsic toughening mechanisms, including crack deflection, fiber bridging, controlled debonding, frictional sliding, and distributed energy dissipation [118]. In contrast, monolithic ceramics typically fail through rapid, unstable crack propagation once a critical flaw is activated. This enhanced damage tolerance underpins the growing deployment of CMCs in extreme environments such as gas-turbine hot sections, hypersonic thermal protection systems, advanced nuclear technologies, and high-temperature industrial components, where sudden failure is unacceptable [119]. Importantly, CMC toughening should not be interpreted as a single mechanism. Instead, it arises from coupled multiscale interactions among the fibers, matrix, interphase, and processing-defined defect populations, consistent with the processing–microstructure framework discussed in previous Section 3.5 [118,119]. A defining characteristic of fiber-reinforced CMCs is that matrix microcracking initiates stress well below ultimate failure. Unlike monolithic ceramics, these cracks are arrested or deflected at the engineered fiber–matrix interphase, which increases crack-path tortuosity and reduces the effective stress intensity at the crack tip. This promotes stable, distributed damage evolution by transferring load to the fibers and enabling gradual stiffness degradation rather than sudden fracture [120]. The stability of this response depends strongly

on interphase shear strength. Interfaces that are too strong suppress sliding and promote brittle fiber fracture, whereas overly weak interfaces reduce load transfer and cause premature fiber disengagement. This balance defines the interphase design window discussed earlier [121].

Among extrinsic toughening mechanisms, fiber bridging is often the primary contributor to crack-growth resistance in continuous-fiber CMCs. Fibers spanning the crack wake generate closure stresses that reduce crack opening and lower the effective driving force for crack extension [122]. The extent of bridging depends on fiber strength, fiber volume fraction, and interfacial sliding resistance. As a result, continuous-fiber systems such as SiC/SiC and C/C can exhibit fracture resistance far greater than that of dense monolithic ceramics [123]. Frictional sliding and fiber pull-out further increase fracture energy by converting elastic strain energy into interfacial frictional work and new surface formation. Controlled debonding allows fibers to slide relative to the matrix, delaying damage localization and suppressing catastrophic failure [124]. Reported differences across studies often arise from variations in processing-induced microstructure, particularly porosity connectivity and interphase degradation, rather than chemistry separately [121–125]. This highlights the need for process-aware interpretation of toughening performance.

Distributed matrix microcracking provides an additional mechanism for damage mitigation in CMCs. Microcrack networks reduce stress concentrations at dominant defects and delay unstable crack growth by distributing strain over a larger process zone. This distributed damage also produces measurable precursors to failure, including stiffness degradation and acoustic activity, enabling structural health monitoring based on acoustic emission, elastic modulus evolution, or electrical resistance changes [126]. These detectable indicators provide a clear advantage over monolithic ceramics and many metallic systems, particularly in safety-critical aerospace and energy applications. Residual thermal stresses generated during processing and cooldown also influence toughening behavior [127]. Thermal expansion mismatch between the fiber and matrix can produce compressive stress fields in the surrounding matrix, increasing the critical stress for crack initiation and stabilizing crack growth [128]. However, residual stress must be carefully controlled. Beneficial compressive states can promote crack deflection and interfacial sliding, whereas excessive mismatch can induce fabrication microcracking and reduce fatigue reliability. SiC/SiC systems offer a favorable balance due to closely matched thermal expansion coefficients, supporting stable residual stress states and improved toughness retention under thermo-mechanical cycling [129].

Interphase engineering is central to maintaining damage tolerance under coupled mechanical and environmental loading. Boron nitride (BN) and multilayer BN/SiC interphases promote crack-tip blunting, stable debonding, and sustained interfacial sliding while offering improved oxidation resistance compared with single-layer designs [130]. Multilayer interphases are therefore an effective approach for retaining interfacial compliance in steam-rich and corrosive environments [131]. At the structural scale, 3D fiber architectures provide greater damage tolerance than 2D laminates. Through-thickness reinforcement in braided and woven preforms suppresses delamination, improves impact resistance, and reduces sensitivity to interlaminar shear failure. These advantages are particularly important in curved and rotating components where multiaxial stress states dominate, and delamination can trigger rapid failure [132].

Environmental stability is inseparable from damage tolerance in CMCs, since extrinsic toughening relies strongly on interfacial sliding and fiber bridging [133]. In SiC-based CMCs, oxidation and volatilization in water vapor-rich environments degrade the interphase and embrittles fibers, suppressing pull-out and bridging mechanisms [134]. In oxide CMCs, oxidation resistance is intrinsically higher, but fiber creep and microstructural

coarsening progressively reduce high-temperature strength retention [135]. To mitigate these degradation pathways, environmental barrier coatings (EBCs), particularly rare-earth silicate systems, have been developed to preserve fiber integrity and maintain interphase functionality under aggressive steam and combustion conditions [136]. These protective strategies ultimately determine whether toughening remains active over service life, explaining why identical architectures can exhibit markedly different durability across environments.

Recent research is expanding CMC damage-tolerance strategies through hierarchical and hybrid designs [137–140]. Nanoscale reinforcements, including graphene derivatives, carbon nanotubes, and nano-SiC, are being investigated to tailor microcracking behavior and improve oxidation resistance at critical interfaces [141]. In parallel, self-healing CMCs incorporating Si- or B-containing phases that form protective oxides *in situ* have demonstrated potential to extend service life under cyclic oxidation by sealing microcracks and restoring barrier performance [142]. Together, these developments reflect a broader shift toward functional microstructural design that couples extrinsic toughening with environmental resistance. A compact summary linking toughening mechanisms with microstructural requirements and environmental sensitivity is provided in Table 5.

Table 5. Dominant extrinsic toughening pathways in CMCs and controlling microstructural requirements.

Toughening Mechanism	Microstructural Requirement	Primary Contribution to Damage Tolerance	Key Limiting Factor
Crack deflection [143]	Compliant engineered interphase, controlled interfacial shear strength	Lowers crack driving force, increases crack-path tortuosity	Interphase oxidation or embrittlement, excessively strong bonding
Fiber bridging [144]	Continuous high-strength fibers, stable interphase response	Generates crack-closure stress, delays crack opening	Fiber degradation, creep, oxidation, weak architecture
Interfacial sliding and debonding [145]	Interphase shear strength within an intermediate window	Major energy dissipation and stable damage evolution	Too strong causes brittle fracture, too weak reduces load transfer
Fiber pull-out	Controlled debond length, stable interfacial friction	High fracture energy absorption	Interphase degradation, fiber surface damage
Distributed matrix microcracking [146]	Controlled matrix continuity and defect population	Strain redistribution and progressive stiffness degradation	Excess microcracking reduces strength, connected porosity accelerates damage
Residual stress toughening [147]	Favorable thermal mismatch and controlled cooling profile	Raises crack initiation stress and stabilizes crack growth	Excess residual stress causes fabrication microcracking

Table 5 summarizes the dominant extrinsic toughening mechanisms in CMCs and links each mechanism to its required microstructural condition. It highlights that crack deflection, bridging, sliding, and pull-out depend strongly on interphase design and fiber integrity, while distributed microcracking and residual stresses control damage stability. The table also identifies key limiting factors, showing that oxidation, creep, excessive bonding, and connected porosity are the primary causes of toughening degradation. Overall, the toughness of CMCs arises from synergistic interactions among matrix microcracking, interfacial debonding, fiber bridging, frictional sliding, and beneficial residual stress fields [144–147]. Together, these coupled mechanisms provide a unique combination of high fracture resistance, progressive damage evolution, and predictable failure behav-

ior, distinguishing CMCs from monolithic ceramics and many metallic alloys [148]. This capacity for stable, non-catastrophic damage progression underpins their growing importance in structural systems operating under extreme temperature, stress, and aggressive environmental conditions.

6. Environmental Stability and Protection Strategies

Environmental stability is a primary determinant of long-term mechanical performance, operational reliability, and certification viability of CMCs in high-temperature service. Even when continuous fibers and engineered interphases provide high fracture resistance and damage tolerance, CMCs remain vulnerable to coupled thermo-chemical degradation under realistic exposure conditions. Key drivers include high-temperature oxidation, steam-assisted volatilization, molten salt or deposit infiltration, and, in certain platforms, irradiation damage [148]. In practice, durability is not governed by intrinsic strength alone but by the ability to preserve the mechanisms that enable damage tolerance, including interfacial sliding, crack deflection, and fiber bridging. Environmental durability must therefore be treated as a coupled material–microstructure–transport problem in which processing-defined pore connectivity, interphase stability, and protective-system integrity collectively control lifetime [149]. This requirement is especially critical for aerospace propulsion, hypersonic vehicles, nuclear systems, and industrial platforms where operating temperatures often exceed 1200–1500 °C and unexpected failure is unacceptable [149,150]. To facilitate mechanistic interpretation, the dominant oxidation/recession process is schematically illustrated in Figure 4a,b, while the progressive failure sequence of environmental barrier coatings (EBCs) under steam cycling is summarized in Figure 4a–e.

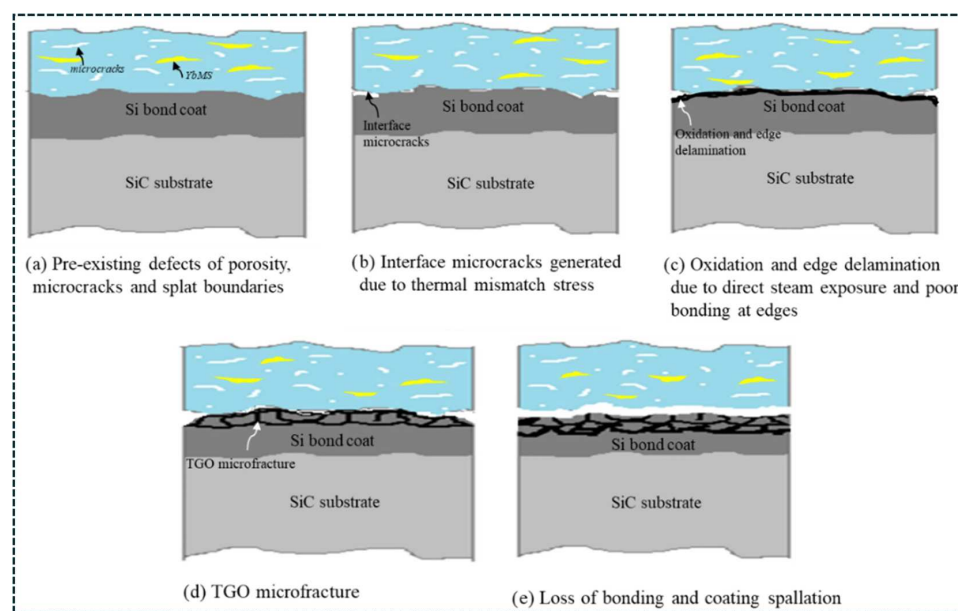


Figure 4. Schematic of damage evolution in APS environmental barrier coatings (EBCs) during steam thermal cycling: (a) pre-existing porosity/microcracks, (b) interface microcrack formation due to thermal mismatch, (c) oxidation and edge delamination, (d) TGO microfracture, and (e) coating debonding/spallation [151].

Non-oxide CMCs, particularly SiC/SiC and C/C, are highly sensitive to oxidation-driven property loss. In SiC-based systems, oxidation initially forms a silica (SiO_2) scale that can provide short-term passivation by limiting oxygen ingress [151]. Under steam-rich combustion environments, however, silica reacts with water vapor to form volatile hydroxide species such as $\text{Si}(\text{OH})_4$, leading to volatilization-driven recession rather than

stable protective-scale growth. As the surface recedes, fibers and interphases become increasingly exposed, accelerating embrittlement and progressively suppressing crack bridging and fiber pull-out. These mechanisms are central to damage tolerance, so their degradation leads to a shift from sliding-controlled graceful failure to brittle fracture behavior [108–152]. If unmitigated, volatilization and interphase oxidation can reduce service life by more than an order of magnitude [153,154]. Carbon-based systems remain stable in inert atmospheres but oxidize at relatively low temperatures of ~500–600 °C, making oxidation protection essential whenever oxygen is present. Oxide-based CMCs, including mullite- and alumina-matrix systems, provide intrinsic oxidation stability in air. However, long-term high-temperature mechanical performance is still constrained by creep and microstructural coarsening, particularly above ~1100 °C, where grain-boundary sliding, fiber deformation, and microstructural evolution gradually reduce load-bearing capability [155]. Thus, while oxide CMCs are less chemically vulnerable than non-oxide systems, maintaining mechanical durability requires careful control of fiber architecture, interphase behavior, and thermal compatibility under sustained loading.

In aero-engine environments, molten deposits represent a severe and often rapid degradation mode. Calcium–magnesium–alumino–silicate (CMAS) deposits can melt and infiltrate porous matrices and EBCs during turbine operation above ~1200 °C, reacting with coating phases and weakening protective layers [156]. CMAS infiltration becomes more damaging when coatings contain cracks or when the underlying composite contains connected porosity networks that promote capillary transport. Under realistic ingestion scenarios involving volcanic ash or desert sand, infiltration accelerates oxidation, induces coating microcracking and delamination, and can significantly shorten the lifetime of SiC-based CMC components [157]. This pathway is directly linked to processing because CVI- and PIP-derived pore connectivity and infiltration pathways strongly influence penetration depth and coating failure susceptibility, as highlighted in previous Section 3.5. In addition, thermally induced crack opening during cyclic exposure promotes crack pumping, increasing deposit penetration depth and amplifying coating/substrate reaction kinetics.

Nuclear applications introduce additional degradation mechanisms. Neutron irradiation can reduce fiber and matrix integrity through defect accumulation, swelling, and microstructural disorder [158]. Interphase coatings may also undergo chemical or structural modification that reduces their ability to support fiber pull-out and crack bridging, thereby suppressing damage tolerance. SiC-based systems generally show relatively strong irradiation resistance due to covalent bonding, but gas accumulation and defect evolution still require rigorous qualification for fission and fusion environments [159]. Durable deployment in nuclear platforms therefore depends not only on high-temperature strength retention but also on long-term microstructural stability under irradiation.

Because environmental degradation directly suppresses toughening retention, protective strategies are essential for CMC deployment. EBCs provide critical protection against oxidation, volatilization-driven recession, and corrosive penetration. Multilayer EBC systems based on rare-earth silicates such as Yb_2SiO_5 and $\text{Yb}_2\text{Si}_2\text{O}_7$ offer water vapor resistance, thermal expansion compatibility with SiC, and chemical stability under turbine-relevant exposure [160]. By shielding fibers and interphases from reactive gases, EBCs preserve interfacial sliding and bridging, which sustain toughness and fatigue resistance. In practical terms, coating integrity directly governs service-life limits and maintenance intervals for hot-section hardware. Accordingly, EBC design must simultaneously suppress (i) transport of steam/deposits through coating defects and (ii) interfacial damage accumulation under thermomechanical cycling.

Coating performance remains limited by thermo-mechanical cycling. Cyclic thermal gradients generate mismatch stresses that drive microcracking, delamination, and spalla-

tion. Thermo-mechanical stress localization is a primary driver for coating cracking and delamination during cyclic service. To illustrate the magnitude and spatial heterogeneity of these driving forces, Figure 5a–d presents representative stress contour predictions for an EBC-coated CMC turbine vane [161]. The distributions of σ_{11} , σ_{22} and σ_{33} show pronounced stress gradients associated with component curvature and thermal expansion mismatch across the coating architecture (Figure 5a–c). High tensile stresses concentrate near free edges and curved regions, which are well-established initiation sites for mud-cracking, interface debonding and edge delamination. The von Mises stress field (Figure 5d) further identifies critical coating zones prone to cyclic damage accumulation, providing mechanistic support for the experimentally observed degradation sequence in steam cycling.

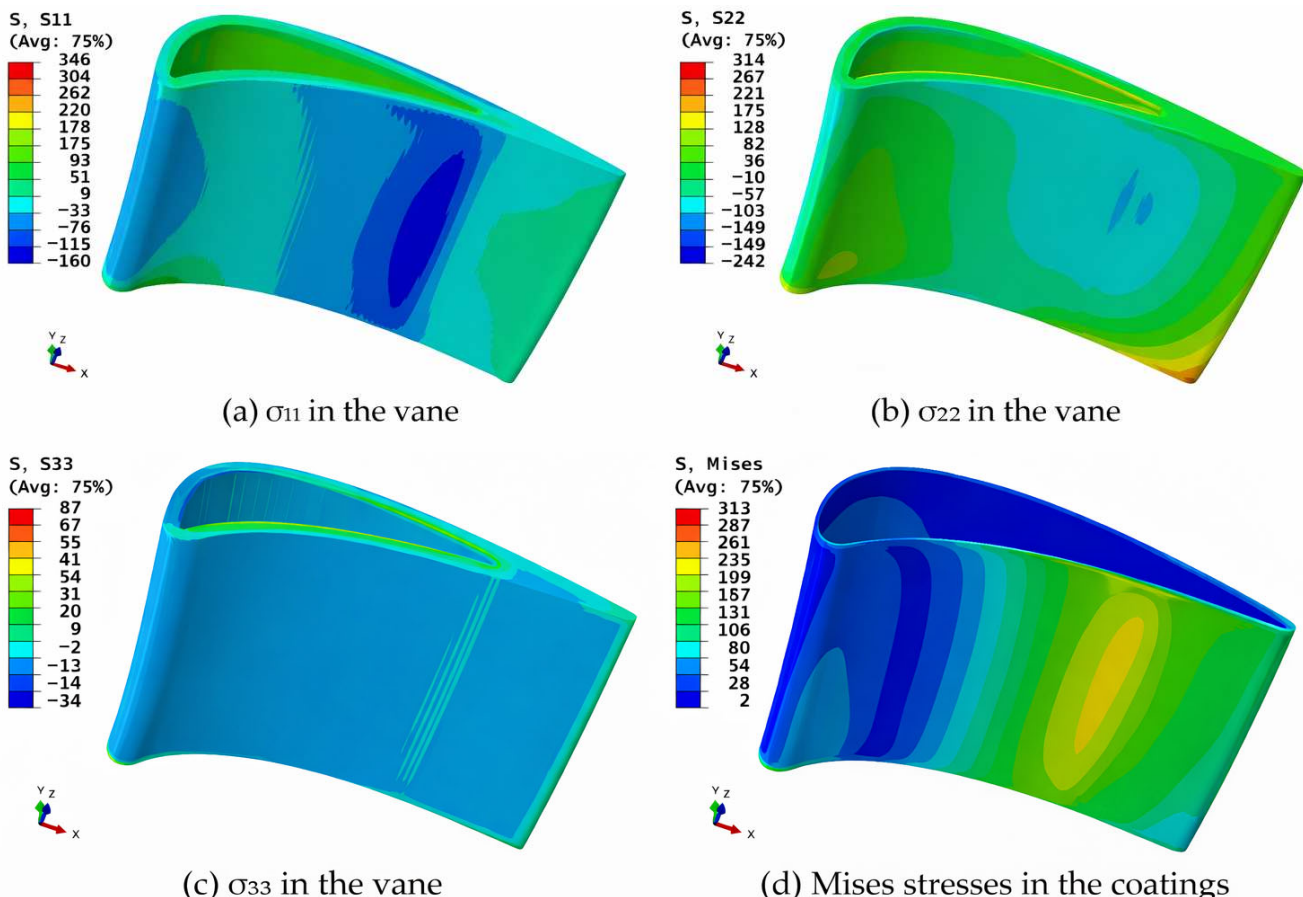


Figure 5. Finite-element predicted thermo-mechanical stress distributions in an EBC-coated CMC turbine vane: (a) σ_{11} , (b) σ_{22} , and (c) σ_{33} stress components in the vane, and (d) von Mises stress distribution in the coating layers, highlighting stress localization regions relevant to crack initiation and delamination under thermal cycling [161].

Further, even small defects can become fast ingress pathways for steam and deposits, so high adhesion, strain tolerance, and defect-tolerant behavior are key design requirements [161]. Previously described Figure 4a–e schematically summarizes the damage evolution sequence of APS EBCs during steam cycling, where pre-existing porosity/microcracks act as initiation sites, followed by interface cracking, TGO-related damage, edge delamination, and eventual coating spallation. Self-healing coating concepts, where microcracks trigger the formation of protective oxides that restore barrier function, have therefore gained increasing attention for extending lifetime under cyclic exposure [162]. Coatings are also complemented by intrinsic strategies, including oxidation-resistant fibers, multilayer or nanostructured interphases, and oxide-coated reinforcement surfaces that improve re-

silence while maintaining interfacial sliding and bridging. In severe turbine and hypersonic environments, Si-rich additives or refractory borides may further improve scale stability and reduce volatilization by modifying oxide chemistry and transport pathways [163].

Corrosion, Volatilization, and Molten-Metal Interaction in Extreme Environments

In addition to oxidation and CMAS-driven coating attack, the long-term reliability of ceramic matrix composites (CMCs) is strongly governed by coupled corrosion, volatilization-driven recession, and molten-metal interactions, which are most severe under extreme heat-flux conditions where multiple reactive species coexist. Such service environments often contain steam-rich combustion gases, molten salts or glassy deposits, and reactive liquid metals, enabling rapid transport, dissolution, and infiltration processes that accelerate microstructural damage beyond that predicted by dry oxidation alone [164,165]. These mechanisms progressively degrade fiber/matrix interphases and restrict the interfacial sliding required for extrinsic toughening, thereby reducing damage tolerance and fatigue resistance.

For SiC-based CMCs, steam-driven volatilization (recession) remains one of the dominant degradation pathways. As schematically summarized in Figure 6a,b, oxidation initially produces a silica (SiO_2) scale that limits oxygen ingress at the SiC/oxide interface (Figure 6a). However, under high-temperature steam, water vapor reacts with the silica layer to form volatile hydroxide species, particularly $\text{Si(OH)}_4(g)$, resulting in continuous silica removal and net material recession (Figure 6b) [166]. This volatilization becomes especially severe under turbine-like conditions involving elevated temperature and high gas velocity, where scale loss is transport-controlled. Progressive thinning reduces the load-bearing cross-section, increases surface roughness, and promotes defect generation during thermal cycling. These defects accelerate oxidant transport and drive interphase recession, suppressing fiber sliding and pull-out mechanisms that underpin fracture resistance and fatigue tolerance [167].

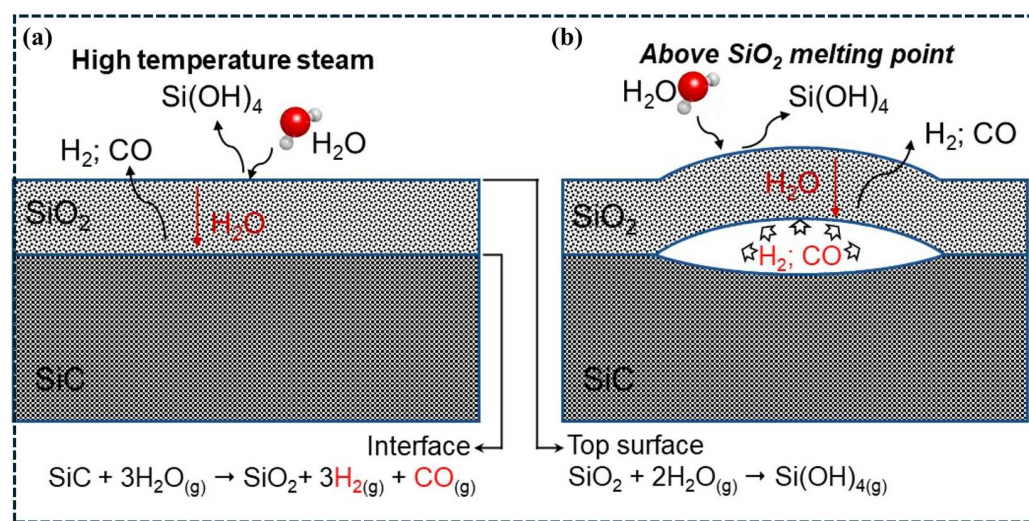


Figure 6. Steam oxidation and recession of SiC: (a) SiO_2 scale formation and (b) volatilization to $\text{Si(OH)}_4(g)$ causing continuous material loss [166].

To support the above steam-recession discussion with experimental evidence, Figure 7a,b presents representative cross-sectional micrographs of a multilayer rare-earth silicate EBC system deposited on a SiC/SiC CMC substrate after water-vapor exposure. The images highlight typical degradation features in steam environments, including the formation of surface-connected mud-crack networks within the topcoat (Figure 7a) and the development of a diffusion/reaction zone at the coating–substrate interface (Figure 7b) [167].

These defects act as transport pathways for steam ingress and accelerate interfacial reactions, thereby promoting coating degradation and increasing the likelihood of delamination during thermal cycling.

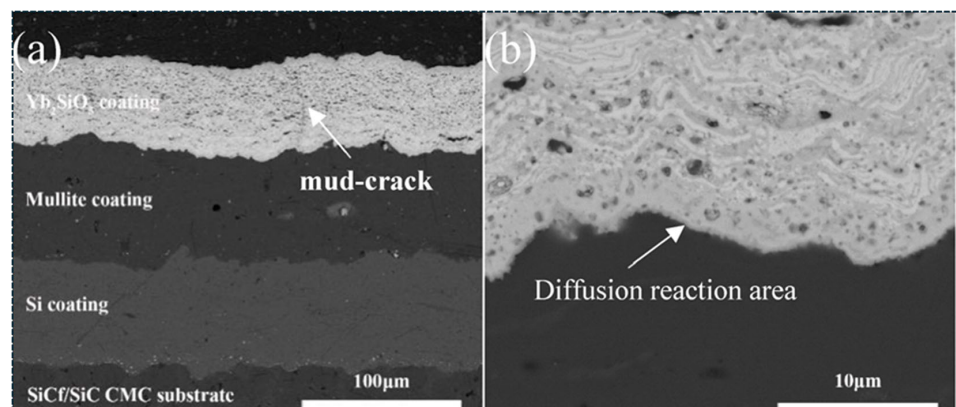


Figure 7. Cross-sectional microstructure of a multilayer rare-earth silicate EBC on SiC/SiC after water-vapor exposure: **(a)** coating architecture showing mud-crack formation in the topcoat and **(b)** higher-magnification view revealing an interfacial diffusion/reaction zone [167].

Beyond CMAS, molten deposit infiltration can involve complex chemistries, including sulfates, chlorides, and mixed silicates, depending on operating conditions and fuel impurities [168]. Once molten, deposits penetrate coating defects and surface-connected porosity, and capillary infiltration is particularly pronounced in CVI- and PIP-derived microstructures where open pore channels may persist after densification. Deposits can subsequently solidify into glassy or crystalline phases that introduce thermal-expansion mismatch stresses, promoting crack opening, delamination, and repeated infiltration during cyclic exposure [169]. Coating spallation then exposes the underlying CMC, triggering rapid oxidation and accelerating fatigue-driven damage accumulation.

Molten-metal interaction is an increasingly important failure mode, particularly under molten aluminum exposure and in environments involving reactive metal vapors or melts during joining, processing, or extreme service [170]. Molten metal attack proceeds through wetting, oxide dissolution, reaction-layer formation, and infiltration along cracks and residual porosity. Once the metal penetrates the composite, it functions both as a chemical reactant and a mechanical wedge, promoting crack opening and accelerating damage coalescence. This is especially detrimental for CMCs because their damage tolerance depends on controlled interphase debonding and sliding [171]. Molten metal infiltration can chemically destabilize the interphase, increase interfacial shear resistance, and effectively lock sliding interfaces, thereby suppressing energy dissipation and triggering premature brittle failure well before bulk oxidation alone would predict.

Importantly, these coupled corrosion, volatilization, and molten-metal mechanisms are strongly microstructure dependent [172]. Connected porosity, permeability, and thermally induced crack opening accelerate transport and infiltration, while residual stress gradients intensify coating delamination and create additional ingress pathways [173]. Processing route therefore directly impacts environmental durability by defining pore morphology, microcrack density, and interphase stability: CVI preserves chemistry but may retain open porosity [174]; PIP can generate shrinkage microcracking unless sufficiently densified; MI reduces porosity but may introduce residual phases that degrade at high temperature; and AM-derived components may exhibit anisotropic defect populations without rigorous post-densification and quality control [175].

Mitigation therefore requires protection strategies beyond conventional oxidation barriers. Multilayer environmental barrier coating (EBC) architectures remain essential,

while next-generation designs increasingly emphasize transport limitation, self-sealing capability, and chemistry tailoring. Dense seal coats suppress infiltration by closing surface-connected porosity [176], while diffusion barrier layers and engineered interlayers stabilize interfaces under coupled thermo-chemical loading. Chemistry optimization can reduce fluxing susceptibility, resist wetting, and improve thermodynamic stability in the presence of molten deposits and reactive metals. Overall, environmental durability should be treated as a coupled material–transport–microstructure design challenge, rather than a surface oxidation issue alone [177]. To consolidate these extreme-environment degradation modes and corresponding mitigation strategies, Table 6 summarizes key mechanisms, vulnerabilities, and protection approaches.

Table 6. Extreme-environment degradation mechanisms in CMCs and mitigation strategies.

Degradation Mode	Service Environment	Primary Mechanism	Key Vulnerabilities	Typical Consequences	Key Mitigation Strategies
Volatilization/recession [178]	Steam-rich combustion (turbines, propulsion)	SiO_2 reacts with $\text{H}_2\text{O} \rightarrow$ volatile species \rightarrow recession	Connected porosity, coating microcracks, interphase exposure	Thickness loss, roughness, crack growth, reduced sliding and pull-out	Multilayer EBCs, steam-resistant topcoats, seal coats, crack-tolerant designs
Molten deposit infiltration (beyond CMAS) [179]	Mixed silicates, sulfates, chlorides	Melt infiltration into defects, fluxing and reactions	Connected porosity, crack pumping during cycling	Delamination, spallation, reaction layers, accelerated oxidation	Dense seal coats, infiltration-resistant EBC chemistries, graded coatings, defect minimization
Molten-metal interaction (e.g., Al) [180]	Molten Al contact, reactive metal exposure	Wetting, dissolution, reaction layers, crack infiltration	Microcracks, open porosity, unstable interphase	Interphase locking, brittle transition, rapid damage accumulation	Wetting-resistant barriers, diffusion interlayers, dense coatings, microstructure densification
Coupled thermo-chemo-mechanical degradation [181]	Thermal cycling with stress and corrosion	Stress-assisted cracking with enhanced transport	Residual stress gradients, interlayer mismatch, weak adhesion	Crack growth, spallation, fatigue strength loss	Compliant bond coats, toughened multilayers, residual stress control, QA and NDE

Table 6 summarizes the dominant extreme-environment degradation modes that control the long-term durability of CMCs beyond conventional oxidation damage. It highlights that volatilization recession, molten deposit infiltration, and molten-metal attack are all accelerated by connected porosity, coating microcracks, and interphase exposure, which directly suppress sliding- and bridging-based toughening. The table also shows that coupled thermo-chemo-mechanical loading amplifies damage through stress-assisted cracking and transport [179–181]. Across all modes, reliability is governed by the interaction between microstructure and transport pathways, not chemistry alone. Accordingly, mitigation requires multilayer EBC systems with seal coats, transport-limiting interlayers, crack-tolerant architectures, and strong QA/NDE control.

7. High-Temperature Applications of CMCs

Ceramic matrix composites (CMCs) have progressed from laboratory-scale systems to qualified engineering materials in sectors where high-temperature capability, mechanical reliability, and damage tolerance must be achieved simultaneously. Their value derives from low density, strength retention above ~ 1200 – 1400 $^{\circ}\text{C}$, and non-catastrophic failure enabled by extrinsic toughening mechanisms. These attributes address key limitations of both metallic superalloys and monolithic ceramics [182]. As engineering targets increasingly prioritize fuel efficiency, emissions reduction, and extended service life, CMCs are emerging as enabling materials for aerospace propulsion, hypersonic platforms, advanced nuclear systems, transportation, and high-temperature industrial infrastructure [183]. Importantly, application success depends on material chemistry. Component viability is governed by manufacturability and defect control (Section 3), retention of interphase-enabled toughening (Section 5), and durability of protective systems under service exposure (Section 6).

7.1. Aerospace Propulsion: Hot-Section Components and Efficiency Gains

The most mature deployment domain for CMCs is aerospace propulsion, where improved temperature capability and reduced cooling requirements deliver direct efficiency and mass benefits. Conventional Ni-based superalloys experience rapid strength loss above ~ 1100 $^{\circ}\text{C}$ and require intensive cooling architecture, which increases complexity and reduces cycle efficiency [184]. In contrast, SiC/SiC CMCs integrated into turbine shrouds, combustor liners, and stationary vanes retain structural capability at $\sim 1300\text{--}1400$ $^{\circ}\text{C}$, supporting higher operating temperatures and reduced cooling-air extraction. This transition to flight-certified SiC/SiC hardware represents system-level adoption rather than incremental material development [185]. Reported comparisons to superalloy analogs indicate $\sim 30\text{--}40\%$ component weight reduction and $\sim 6\text{--}8\%$ fuel-use reduction, contingent on long-term durability of environmental barrier coatings (EBCs) under steam volatilization and deposit attack (Section 6) [186].

7.2. Hypersonic and Re-Entry Systems: Ultra-High Temperature Survivability

Hypersonic flight and atmospheric re-entry impose heat loads that can exceed ~ 2000 $^{\circ}\text{C}$, which pushes metallic systems beyond melting and creep limits [187]. Carbon/carbon (C/C) composites and UHT-CMCs are therefore leading candidates for components such as leading edges, control surfaces, and thermal protection structures, where both thermal shock resistance and erosion tolerance are required [187,188]. UHT-CMCs incorporating carbides and borides such as ZrB_2 and HfC extend survivability under combined heating and erosion, making them relevant to high-speed defense and aerospace applications [189]. However, UHT-CMC deployment remains constrained by oxidation susceptibility and processing scalability, which links adoption directly to coating solutions and densification strategies (Section 3). A practical mapping between CMC classes, component roles, and operating windows is summarized in Table 7.

Table 7. Representative CMC material classes and aeronautical application windows.

CMC Type	Components	Temperature	Advantages
SiC/SiC [189]	Turbine shrouds, combustor liners, vanes	1300–1500 $^{\circ}\text{C}$	High strength, oxidation resistance, reduced cooling demand
C/C [190]	Rocket nozzles, thermal protection, friction components	2000–2500 $^{\circ}\text{C}$ (in inert environments)	Extreme thermal shock resistance, lightweight
Oxide–Oxide CMCs [191]	Exhaust structures, industrial furnace parts	$\leq 1100\text{--}1200$ $^{\circ}\text{C}$	Excellent oxidation resistance, lower cost
UHTCMCs (ZrB_2 , HfC reinforced) [192]	Hypersonic leading edges, high-speed control surfaces	$>2000\text{--}3000$ $^{\circ}\text{C}$	Ultra-high temperature survival, erosion resistance

Table 7 reflects a temperature–environment–manufacturing selection logic. SiC/SiC provides the best balance of turbine-relevant capability and manufacturability but requires robust EBC durability. C/C offers unmatched thermal shock tolerance but demands strong oxidation protection. Oxide–oxide systems are chemically stable and cost-favorable yet limited by creep and strength loss at higher temperatures. UHT-CMCs enable the highest temperature operation, though scalability and oxidation remain limiting barriers.

7.3. Nuclear Energy Systems: Irradiation Compatibility and High-Temperature Efficiency

CMCs are also strong candidates for advanced nuclear energy systems, including gas-cooled fission concepts and fusion devices, where materials must tolerate chemically aggressive coolants, irradiation damage, and cyclic high-temperature loading. SiC/SiC composites are leading candidates for fuel cladding, control components, and heat exchangers due to low neutron absorption, limited radioactive activation, and irradiation-tolerant stability [193]. Chemical inertness can also reduce contamination risk and improve safety margins. In fusion-relevant high heat-flux regions, UHT-CMCs are under active study because they extend temperature capability beyond Ni-based alloys and some refractory metal solutions [194]. Qualification remains limited by uncertainty in long-term irradiation effects on fiber strength, interphase stability, and damage tolerance, requiring coupled exposure testing and validated predictive models [195].

7.4. Transportation: Braking and Thermal Hardware

In transportation, CMC adoption is most established in braking systems where repeated high-temperature cycles demand stable friction and thermal shock tolerance. C/C composites dominate aerospace and motorsport braking because they maintain integrity under severe deceleration cycles while reducing mass and wear relative to metallic solutions. Beyond braking, SiC-based CMCs are being evaluated for high-temperature exhaust and lightweight structural hardware, particularly where thermal cycling drives fatigue and distortion in metals [196,197]. The key functional advantage is predictable damage evolution under cyclic thermal loading.

7.5. Industrial Infrastructure and Clean Energy Systems

CMCs offer value in industrial systems where combined thermal and chemical exposure accelerates metallic degradation. Heat exchangers, radiant tubes, burners, and casting hardware can benefit from CMC corrosion resistance and thermal stability, reducing maintenance frequency and extending uptime. As SiC-based radiant tubes resist carburization and sulfur attack in furnace environments, they often deliver longer life than metallic counterparts [198]. Clean energy platforms such as hydrogen production reactors and concentrated solar receivers also require materials that resist oxidation and corrosion at elevated temperatures. In these systems, oxide-based CMCs can be attractive due to oxidation stability at moderate operating windows [199]. In many applications, lifecycle cost is decisive, where higher initial material cost can be offset by reduced cooling needs, longer maintenance intervals, and lower downtime [200]. Table 8 summarizes representative system-level benefits from CMC substitution.

Table 8. Representative performance benefits enabled by CMC substitution.

Component	Conventional Material	Performance Improvement	References
Turbine shroud/combustor liner	Nickel-based superalloys	Lower fuel use, reduced weight, and extended component lifespan benefits.	[201]
Brake discs (aerospace/racing)	Cast iron/steel alloys	40–60% weight reduction, high wear resistance, stable braking above 1500 °C.	[202]
Thermal protection for hypersonic	Metals/coatings	Survive above 2000 °C without melt-induced structural failure.	[203]
Nuclear heat exchangers	Stainless steels/Ni alloys	Longer corrosion life, reduced neutron activation, and improved operational safety margins.	[204]

Table 8 confirms that the value proposition of CMCs is application-specific. Propulsion benefits are dominated by efficiency gains from reduced cooling-air extraction. Braking benefits are governed by thermal shock tolerance and friction stability. Hypersonic benefit is survival beyond metallic thermal limits. Nuclear benefits are irradiation-compatible stability and reduced activation. Across all categories, benefit retention depends on processing reproducibility and environmental protection, confirming that QA and EBC durability are enabling constraints rather than secondary considerations.

7.6. Rising Demand for Extreme Environment Structural Materials

Demand for extreme-environment materials is expected to increase with next-generation propulsion cycles, hypersonic structures, and advanced nuclear platforms. Future engines seek higher operating temperatures with reduced cooling architecture, while hypersonic systems push combined thermal and mechanical loading toward ~ 2500 $^{\circ}\text{C}$ [205]. In parallel, SiC-based CMCs are expected to expand in nuclear systems supporting high-temperature hydrogen production and low-carbon energy conversion [206]. Continued progress in scalable processing, EBC robustness, and interphase stability will determine whether CMCs transition from high-value niche deployments to broader industrial adoption.

8. Recent Advances and Industrial Trends

In the past decade, CMCs have progressed from laboratory-scale innovations to industrially deployed high-temperature structural materials. Research priorities have shifted from demonstrating damage tolerance under idealized conditions to enabling service-relevant durability, manufacturing scalability, and multifunctionality such as self-healing and self-sensing under coupled thermo-chemo-mechanical exposure. These priorities are driven by application demands in aerospace propulsion, hypersonic systems, defense platforms, nuclear technologies, and sustainable energy infrastructure, where components must combine extreme-environment survivability with cost and certification constraints [205]. Many recent advances are therefore best understood as targeted responses to the coupled challenges discussed in Sections 3–6, including processing-driven defect control, retention of interphase-enabled toughening, and reliability of environmental protection systems.

8.1. Interphase and Fiber Engineering for Durability Retention

Interphase and fiber design remain central because long-term toughness retention depends on preserving interfacial sliding and crack bridging in aggressive environments. Conventional PyC and BN interphases provide compliance and sliding but degrade by oxidation or hydrolysis in steam-rich service, which reduces pull-out efficiency and drives a transition toward brittle fracture [206]. As a result, current efforts focus on oxidation-tolerant interphases, including oxide-compatible multilayer nitride–oxide architectures and rare-earth phosphate-based designs that retain sliding functionality after prolonged exposure [207]. Multilayer interphases that combine crystalline and amorphous layers are particularly effective because they preserve frictional response while improving chemical stability against volatilization and corrosion. In parallel, advances in SiC fiber quality, including grain-boundary chemistry optimization and reduced oxygen impurities, have improved creep resistance and retained strain-to-failure above ~ 1400 $^{\circ}\text{C}$, supporting longer service intervals in aviation hot-section environments [208]. Together, these developments directly address the key limitation that toughening mechanisms degrade under service exposure by designing interphase and fiber chemistry for durability rather than only initial performance.

8.2. Self-Healing Coatings and Matrices as Damage-Tolerant Protection

A second major trend is the integration of self-healing functionality into coatings and matrices. Microcracking during service is unavoidable due to thermal cycling and stress gradients, particularly in coated non-oxide CMCs. Instead of eliminating cracks, self-healing strategies aim to restore barrier performance after cracking occurs. Borosilicate or silicate additives in SiC matrices and coating layers can seal microcracks during heating, limiting oxidant and steam transport [209]. Self-healing EBC concepts therefore offer a route to maintain protection under thermomechanical fatigue, with reported multi-fold lifetime improvements under severe turbine exposure [210]. This approach aligns with the CMC design philosophy by allowing controlled damage while preventing damage from evolving into rapid environmental degradation.

8.3. Expansion of UHT-CMCs for Hypersonic and Deep-Space Environments

The development of UHT-CMCs is accelerating for platforms exposed to 2500–3000 °C, ablation, and erosive flow. Carbide and boride reinforcement systems, including SiC-coated carbon fibers and reinforcements based on HfC and ZrB₂, are being combined with dense boride-rich matrices produced via spark plasma sintering or reactive melt infiltration to improve load-bearing capability and resistance to oxidative ablation [211]. In these systems, retaining fiber sliding under Mach 5+ thermo-mechanical exposure remains essential, making interphase stability a survival requirement rather than only a toughness design element. Progress in UHT-CMCs therefore reflects the convergence of densification science, interphase stability, and environmental protection, not chemistry improvement alone.

8.4. Multifunctional CMCs for Self-Sensing and Integrated Monitoring

A strong industrial direction is the development of multifunctional CMCs with embedded sensing capability for structural health monitoring. Conductive networks, piezoelectric phases, and fiber-optic sensors enable real-time measurement of temperature, strain, and damage progression, supporting predictive maintenance and reducing inspection burden. Such self-sensing architectures are especially valuable in aviation and nuclear systems where certification requires reliable, evidence-based life management [212]. This trend also leverages the intrinsic advantage of CMCs, where progressive stiffness degradation and coating damage provide measurable precursors that can be tracked during service.

8.5. Digital Manufacturing: AM, Automation, and Hybrid Densification

Manufacturing advances increasingly emphasize digital workflow integration, linking architecture design, process monitoring, and qualification into a connected production pipeline. AM enables geometries that are difficult to realize using conventional textile routes, including lattices, graded porosity regions, and embedded channels. Direct ink writing, stereolithography of ceramic-loaded resins, and binder jetting are among the most actively explored methods [213–215]. However, the key industrial development is the emergence of hybrid AM workflows such as AM + CVI and AM + PIP, which enable improved microstructure control while reducing cycle time and energy consumption [214,215]. In parallel, automated textile manufacturing, including robotic braiding and programmable 3D weaving, enables scalable production of stress-optimized fiber architectures with reduced labor intensity and improved defect control [216].

8.6. Cost Reduction, Supply Chain Maturity, and Certification Evolution

Large-scale adoption remains constrained by cost and certification. Improvements in high-purity fiber production, optimized matrix precursors, shortened infiltration cycles, recyclable tooling, and sol-gel-derived polymer routes are improving the economic feasibility

of CMC manufacturing [217]. At the same time, supply chain maturation through industrial partnerships reduces procurement risk and supports scaling beyond niche defense and aerospace markets. Certification approaches are also evolving, with probabilistic lifting and digital twin frameworks that incorporate oxidation-assisted fatigue, creep–fatigue interaction, thermal shock, and coating degradation kinetics to enable longer inspection intervals while maintaining safety margins [218]. From a sustainability perspective, CMC deployment can improve turbine and industrial thermal efficiency by reducing cooling-air extraction and enabling higher operating temperatures, supporting reduced fuel consumption and emissions [219]. These combined developments explain the accelerating shift in CMCs from specialized high-value applications toward broader commercial and industrial integration. To summarize representative recent directions in SiC-based CMC advancement, Table 9 compiles studies spanning self-healing concepts, oxidation resistance, AM processing, and EBC development.

Table 9. Recent advances in SiC-based CMCs and enabling technologies.

Researcher	Description	References
Paladugu et al.	Self-healing mechanisms in ceramic composites for high-temperature aerospace applications.	[220]
Xu et al.	SiC/SiC–SiHfBCN composites with enhanced oxidation resistance for hypersonic thermo-structural applications.	[221]
Park et al.	$\text{C}_\text{f}/\text{SiC}$ composites retaining exceptional flexural strength and thermomechanical performance up to 2000 °C for UHT applications.	[222]
Wang et al.	Recent advances in SiC ceramic matrix composites for aerospace, including processing, toughness, and high-temperature performance.	[223]
Qian et al.	Overview of rare earth silicate environmental barrier coatings protecting CMCs in hot, oxidative, and corrosive environments.	[224]
Liu et al.	Additive manufacturing of continuous fiber SiC/SiC composites achieving ultra-high strength and toughness in ceramic matrix systems.	[225]

Table 9 shows that recent progress in SiC-based CMCs is driven by three tightly coupled directions: improving durability through self-healing concepts and oxidation-resistant chemistries, strengthening environmental stability through advanced rare-earth silicate EBCs, and expanding manufacturability through additive and hybrid processing routes.

9. Challenges and Research Gaps

Despite major progress and growing industrial deployment, CMCs still face scientific, technological, economic, and regulatory barriers that limit broader adoption in high-temperature structural service. A persistent limitation across aerospace, nuclear, industrial, and clean-energy platforms is the lack of fully predictive capability linking processing-defined microstructure, environment-driven degradation, and long-term mechanical reliability [226]. Coupled thermo-mechanical loading and environmental attack remain insufficiently quantified over service-relevant timescales, which restricts confidence in lifetime prediction and certification [227]. Environmental durability remains the dominant technical constraint, especially for SiC-based CMCs exposed to steam, corrosive combus-

tion species, and molten deposits. While EBCs are essential, they introduce additional failure routes such as thermal mismatch stresses, cracking, spallation, and recession. Once protective integrity is compromised, oxidants penetrate rapidly, interphases embrittle, and extrinsic toughening mechanisms such as sliding, pull-out, and bridging are progressively suppressed [226–228]. As a result, lifetime is governed by toughening retention rather than initial toughness. Oxide CMCs provide improved oxidation stability, but above ~ 1100 °C they are limited by creep, fiber coarsening, and time-dependent microstructural evolution, reducing suitability for sustained propulsion-relevant loading [229]. A major research gap is the mechanistic understanding of damage evolution under combined oxidation, volatilization, deposit infiltration, and cyclic stress. In situ high-temperature characterization, including synchrotron X-ray imaging and advanced electron microscopy, is critical for quantifying interphase degradation, microcrack evolution, and transport pathways.

Scalability and manufacturing cost remain major adoption barriers. Conventional densification methods (CVI, PIP, MI) are cycle-time intensive and process sensitive, with thick or complex components often requiring weeks to months of densification. Strict control is required to avoid pore isolation, infiltration gradients, and interphase damage. Fiber preforms remain expensive and contribute substantially to the cost. Although hybrid processing and AM show promise, industrial-scale automation, reproducible process control, and mature supply networks are still developing. Adoption beyond aerospace into automotive, energy, and industrial infrastructure will require step-change cost reduction without sacrificing reliability [230]. This also demands a quantitative understanding of how processing-driven defect populations, including porosity connectivity, microcrack distributions, interphase variability, and fiber misalignment, translate into strength scatter and fatigue variability.

Certification and quality assurance are challenging because CMCs do not behave as monolithic materials. Distributed damage evolution, nonlinear stress-strain response, and architecture-dependent performance complicate inspection and lifting. Conventional deterministic safety factors are often overly conservative or insufficiently representative, motivating probabilistic reliability frameworks and degradation models tailored to CMCs [231]. Harmonized qualification protocols, improved NDE, and standardized defect-tolerance criteria are therefore essential. Digital thread approaches linking process history, inspection results, service exposure, and predictive models offer a scalable route to certification confidence.

Design methodologies also require advancement. CMCs must be engineered as integrated systems in which matrix chemistry, fiber architecture, interphase response, porosity morphology, and reinforcement topology are optimized together. Many design rules remain qualitative and do not translate into quantitative manufacturing-control targets. Multi-objective optimization is needed to balance stiffness, toughness, creep resistance, fatigue durability, oxidation performance, and coating compatibility [230–232]. Defect sensitivity further complicates design since pore clusters, fiber misalignment, and interphase thickness variability can shift fracture mechanisms and sharply reduce durability. Progress increasingly depends on computational tools, including microstructure-resolved simulations, uncertainty quantification, and AI-assisted optimization, particularly for architecture tailoring in AM-enabled components [232].

Joining and repairing remain critical bottlenecks, especially for large-scale adoption. Current high-temperature joining methods such as mechanical fastening and brazing can introduce thermal mismatch, stress concentrations, and defect-sensitive joints that become system-level constraints. Key gaps include robust ceramic–ceramic and ceramic–metal joining strategies, field-compatible repair methodologies, and regeneration approaches for degraded EBCs that restore protection without full replacement [233]. Repairable, maintainable CMC systems are essential for lowering lifecycle costs and improving operational

availability. Sustainability is an emerging constraint. Traditional CMC manufacturing relies on energy-intensive thermal cycles and precursor chemistries with significant lifecycle emissions. Future opportunities include greener processing routes, lower-emission densification, recyclable tooling, circular handling of composite waste, and renewable-energy integration into manufacturing [234]. Several emerging technologies directly address these gaps. UHT-CMCs extend the operating envelope for hypersonic and extreme-energy platforms. Smart CMCs with embedded sensing enable real-time health monitoring and predictive maintenance. Self-healing matrices and coatings maintain barrier integrity under cyclic damage. AM enables complex architecture with internal cooling and graded reinforcement aligned with spatially varying loads [231]. The strongest transformational opportunity lies in digital intelligence. Machine learning for defect prediction, process optimization, and lifetime forecasting can improve reproducibility and directly support certification. When coupled with mechanistic modeling of fracture, creep, and oxidation transport and embedded within probabilistic reliability frameworks, AI-enabled workflows can enable design-for-reliability strategies where microstructure, defects, and performance are optimized together under uncertainty [231,232]. Ultimately, the convergence of environmental chemistry, mechanics, materials science, and digital manufacturing will determine whether CMCs expand beyond high-value aerospace applications into broadly adopted structural solutions.

10. Conclusions and Future Directions

Ceramic matrix composites (CMCs) have emerged as a transformative class of high-temperature structural materials capable of operating where conventional metallic alloys and monolithic ceramics fail. By combining high-strength continuous ceramic fibers with engineered ceramic matrices and compliant interphase layers, CMCs deliver a unique balance of lightweight structural efficiency, high-temperature strength retention, enhanced fracture toughness, and non-catastrophic damage evolution. Unlike monolithic ceramics that fracture abruptly by unstable crack propagation, CMCs dissipate energy through extrinsic mechanisms such as crack deflection, fiber bridging, interfacial sliding, and fiber pull-out, enabling progressive stiffness degradation and residual load-bearing capacity. These attributes have enabled their deployment in aerospace propulsion hot sections, thermal protection systems, nuclear energy technologies, automotive braking, and high-temperature industrial components, where reliability under extreme thermo-mechanical loading is essential.

Despite these achievements, several barriers still limit broader adoption. Environmental durability remains a critical challenge for non-oxide CMCs in steam-rich, oxidizing, and deposit-containing environments because degradation of fibers, interphases, and protective coatings can suppress sliding- and pull-out-based toughening and drive brittle transitions. Manufacturing scalability and economic viability are also constrained by expensive high-purity fibers, slow and energy-intensive densification cycles, and process-sensitive defect populations (porosity connectivity, interphase variability, and fiber misalignment) that increase property scatter and complicate certification. In addition, qualification and quality assurance remain demanding because CMCs exhibit nonlinear behavior and distributed damage evolution, requiring advanced NDE approaches, probabilistic lifing strategies, and service-representative testing; joining, repair, and maintainability (including EBC regeneration) also remain key gaps for long-life industrial deployment.

Future progress will depend on integrated strategies that link processing, microstructure control, environmental protection, and predictive intelligence. Scalable hybrid manufacturing pathways—combining automation, advanced textiles, and additive manufacturing with optimized densification—must be coupled with robust, crack-tolerant envi-

ronmental barrier coatings, self-sealing/self-healing protection concepts, and interphase architectures that retain compliance under harsh exposure. At the same time, physics-based modeling, probabilistic life prediction, and AI-enabled digital twins will increasingly support defect prediction, process optimization, and accelerated qualification by connecting manufacturing history to performance and durability outcomes. With continued advances in coating durability, manufacturability, and digital design/monitoring frameworks, CMCs are expected to expand from specialized aerospace and defense applications into broader commercial adoption across transportation, clean energy, and industrial infrastructure, enabling safer, lighter, and more energy-efficient high-temperature systems.

Author Contributions: Conceptualization, S.K.S., S.G., S.M. and L.K.S.; methodology, S.K.S., L.K.S., M.S., Y.S. and M.S.; software, S.K.S.; validation, S.K.S., S.G. and M.S.; formal analysis, S.G., S.M., S.S. and B.S.; investigation, S.K.S., L.K.S. and S.G.; resources, S.K.S., L.K.S., Y.S. and M.S.; data curation, S.K.S., S.G. and S.M.; writing—original draft preparation, S.K.S.; writing—review and editing, S.K.S., S.G., S.M. and B.S.; visualization, S.K.S. and L.K.S.; supervision, S.S. and B.S.; project administration, S.K.S.; funding acquisition, S.G. and S.M. All authors have read and agreed to the published version of the manuscript.

Funding: This research received no external funding.

Data Availability Statement: The original contributions presented in this study are included in the article. Further inquiries can be directed to the corresponding author(s).

Conflicts of Interest: The authors declare no conflicts of interest.

References

1. Dorfman, M.R.; Dwivedi, G.; Dambra, C.; Wilson, S. Perspective: Challenges in the aerospace marketplace and growth opportunities for thermal spray. *J. Therm. Spray Technol.* **2022**, *31*, 672–684. [\[CrossRef\]](#)
2. Kaur, D.P.; Raj, S.; Bhandari, M. Recent advances in structural ceramics. In *Advanced Ceramics for Versatile Interdisciplinary Applications*; Elsevier: Amsterdam, The Netherlands, 2022; pp. 15–39.
3. Raj, R. Fundamental research in structural ceramics for service near 2000 C. *J. Am. Ceram. Soc.* **1993**, *76*, 2147–2174. [\[CrossRef\]](#)
4. Wiederhorn, S.M. Brittle fracture and toughening mechanisms in ceramics. *Annu. Rev. Mater. Sci.* **1984**, *14*, 373–403. [\[CrossRef\]](#)
5. Wang, Y.-S.; Wang, X.-Z.; Wu, S.; Song, Q.-Z.; Long, X.; Wang, Y.-D. Effect and mechanism analysis of free carbon on the oxidation behaviour of SiC fibres. *Ceram. Int.* **2023**, *49*, 35488–35495. [\[CrossRef\]](#)
6. Karadimas, G.; Salonitis, K. Ceramic matrix composites for aero engine applications—A review. *Appl. Sci.* **2023**, *13*, 3017. [\[CrossRef\]](#)
7. Kabel, J.; Hosemann, P.; Zayachuk, Y.; Armstrong, D.E.J.; Koyanagi, T.; Katoh, Y.; Deck, C. Ceramic composites: A review of toughening mechanisms and demonstration of micropillar compression for interface property extraction. *J. Mater. Res.* **2018**, *33*, 424–439. [\[CrossRef\]](#)
8. Maqbool, M.; Bashir, A.; Usman, A.; Khurram, M.; Aftab, W.; Li, Y.; Zou, R. 3D interconnected boron nitride macrostructures and derived composites for thermal energy regulation. *Adv. Funct. Mater.* **2025**, *35*, 2414042. [\[CrossRef\]](#)
9. Xu, X.; Guo, Y.; Shen, Z.; Liu, B.; Yan, F.; Zhong, N. Aramid Fiber-Reinforced Plastics (AFRPs) in Aerospace: A Review of Recent Advancements and Future Perspectives. *Polymers* **2025**, *17*, 2254. [\[CrossRef\]](#)
10. Gao, R.; Wang, S.; Zhou, T.; Jiang, T.; Lu, L.; Wen, Q.; Tao, S.; Xiong, X. Research Progress on Ultrahigh-Temperature Ceramics Modified C/C Composites. *Materials* **2025**, *18*, 3891. [\[CrossRef\]](#)
11. Chang, J.S.; Facchetti, A.F.; Reuss, R. A circuits and systems perspective of organic/printed electronics: Review, challenges, and contemporary and emerging design approaches. *IEEE J. Emerg. Sel. Top. Circuits Syst.* **2017**, *7*, 7–26. [\[CrossRef\]](#)
12. Ling, Z.; Yang, W.; Chen, W.; Fu, Z. Recent Advances in Understanding the Corrosive Effects of Molten Aluminum on Structural Materials and Protective Strategies: A Comprehensive Review. *Mater. Today Commun.* **2025**, *47*, 113249. [\[CrossRef\]](#)
13. Hu, Z.; Liu, L.; Wang, X.; Lu, H.; Zheng, Q.; Gao, Y.; Wang, J.; Qi, Y.; Han, C.; Li, W. In Situ Integration of Rapid Ion-Diffusion Interlayers on Cu Current Collectors toward Ultrafast Anode-Free Sodium Metal Batteries. *ACS Nano* **2025**, *19*, 23193–23208. [\[CrossRef\]](#)
14. Wang, J.; Zhang, J.; Cheng, G.; Zhang, K.; Liu, X. Performance and mechanism of tetracycline removal by peroxyomonosulfate-assisted double Z-scheme LaFeO₃/g-C₃N₄/ZnO heterojunction under visible light drive. *Environ. Technol. Innov.* **2025**, *39*, 104302. [\[CrossRef\]](#)

15. Jayan, K.D. Recent Advances in Ultra-High-Temperature Ceramic Coatings for Various Applications. In *Ceramic Coatings for High-Temperature Environments: From Thermal Barrier to Environmental Barrier Applications*; Springer: Cham, Switzerland, 2023; pp. 409–440.

16. Sadavar, S.V.; Lee, S.; Park, S. Advancements in asymmetric supercapacitors: From historical milestones to challenges and future directions. *Adv. Sci.* **2024**, *11*, e2403172. [\[CrossRef\]](#) [\[PubMed\]](#)

17. Chen, Z.; Xu, C.; Chen, X.; Huang, J.; Guo, Z. Advances in electrically conductive hydrogels: Performance and applications. *Small Methods* **2025**, *9*, 2401156. [\[CrossRef\]](#) [\[PubMed\]](#)

18. Lee, J.; Ni, J.; Singh, J.; Jiang, B.; Azamfar, M.; Feng, J. Intelligent maintenance systems and predictive manufacturing. *J. Manuf. Sci. Eng.* **2020**, *142*, 110805. [\[CrossRef\]](#)

19. Abbas-Abadi, M.S.; Tomme, B.; Goshayeshi, B.; Mynko, O.; Wang, Y.; Roy, S.; Kumar, R.; Baruah, B.; De Clerck, K.; De Meester, S.; et al. Advancing textile waste recycling: Challenges and opportunities across polymer and non-polymer fiber types. *Polymers* **2025**, *17*, 628. [\[CrossRef\]](#)

20. Li, M.; Tunca, B.; Van Meerbeek, B.; Vleugels, J.; Zhang, F. Tough and damage-tolerant monolithic zirconia ceramics with transformation-induced plasticity by grain-boundary segregation. *J. Eur. Ceram. Soc.* **2023**, *43*, 2078–2092. [\[CrossRef\]](#)

21. Sengupta, P.; Manna, I. Advanced high-temperature structural materials in petrochemical, metallurgical, power, and aerospace sectors—An overview. In *Future Landscape of Structural Materials in India*; Springer: Singapore, 2022; pp. 79–131.

22. Binner, J.; Porter, M.; Baker, B.; Zou, J.; Venkatachalam, V.; Diaz, V.R.; D'ANgio, A.; Ramanujam, P.; Zhang, T.; Murthy, T.S.R.C. Selection, processing, properties and applications of ultra-high temperature ceramic matrix composites, UHTCMCs—A review. *Int. Mater. Rev.* **2020**, *65*, 389–444. [\[CrossRef\]](#)

23. Alizadeh, M.; Nodehi, M.; Salmanpour, S.; Karimi, F.; Sanati, A.L.; Malekmohammadi, S.; Zakariae, N.; Esmaeili, R.; Jafari, H. Properties and recent advantages of N, N'-dialkylimidazolium-ion liquids application in electrochemistry. *Curr. Anal. Chem.* **2022**, *18*, 31–52. [\[CrossRef\]](#)

24. Peters, A.B.; Zhang, D.; Chen, S.; Ott, C.; Oses, C.; Curtarolo, S.; McCue, I.; Pollock, T.M.; Eswarappa Prameela, S. Materials design for hypersonics. *Nat. Commun.* **2024**, *15*, 3328. [\[CrossRef\]](#) [\[PubMed\]](#)

25. Manikandan, S.G.K.; Kamaraj, M.; Jebasihamony, C. Review on Self-Healing Thermal Barrier Coatings for Space Applications. *Mater. Perform. Charact.* **2021**, *10*, 790–818. [\[CrossRef\]](#)

26. Wang, P.; Liu, F.; Wang, H.; Li, H.; Gou, Y. A review of third generation SiC fibers and SiCf/SiC composites. *J. Mater. Sci. Technol.* **2019**, *35*, 2743–2750. [\[CrossRef\]](#)

27. Jeielayaganga, V.; Keerthiga, R.; Venkatesh, M. Recent progress in sustainable energy storage using activated carbon from biowaste for high-performance supercapacitors: A review. *Mod. Electron. Mater.* **2025**, *11*, 65–80. [\[CrossRef\]](#)

28. Wadsworth, J.; Ruano, O.A.; Sherby, O.D. Denuded zones, diffusional creep, and grain boundary sliding. *Met. Mater. Trans. A* **2002**, *33*, 219–229. [\[CrossRef\]](#)

29. Tjong, S.; Mai, Y.-W. Processing-structure-property aspects of particulate-and whisker-reinforced titanium matrix composites. *Compos. Sci. Technol.* **2008**, *68*, 583–601. [\[CrossRef\]](#)

30. Li, M.; Wang, P.; Boussu, F.; Soulat, D. A review on the mechanical performance of three-dimensional warp interlock woven fabrics as reinforcement in composites. *J. Ind. Text.* **2022**, *51*, 1009–1058. [\[CrossRef\]](#)

31. Liu, F.; Fan, C.; Wang, B.; Zhou, C.; Chen, Z. Comparative study of interfacial debonding mechanism of fiber pull-out in magnesium phosphate cementitious composites. *J. Build. Eng.* **2025**, *102*, 111901. [\[CrossRef\]](#)

32. Hong, W.; Pang, X.; Yan, H.; Li, L.; Zhang, Z. Actively-controlled PyC interphase failure mechanisms in C/SiC composite revealed using micro-mechanical interfacial testing. *Ceram. Int.* **2025**, *51*, 3654–3664. [\[CrossRef\]](#)

33. Naslain, R.R.; Paillet, R.J.; Lamon, J.L. Single-and multilayered interphases in SiC/SiC composites exposed to severe environmental conditions: An overview. *Int. J. Appl. Ceram. Technol.* **2010**, *7*, 263–275. [\[CrossRef\]](#)

34. Cugnoni, J.; Amacher, R.; Kohler, S.; Brunner, J.; Kramer, E.; Dransfeld, C.; Smith, W.; Scobie, K.; Sorensen, L.; Botsis, J. Towards aerospace grade thin-ply composites: Effect of ply thickness, fibre, matrix and interlayer toughening on strength and damage tolerance. *Compos. Sci. Technol.* **2018**, *168*, 467–477. [\[CrossRef\]](#)

35. Zhang, Y.; Zhang, W.; Zhang, J.; Cao, W.; Zhang, L.; Wang, D. Thermo-mechanical optimization of alkali activated materials: Synergistic fiber strategy for high-temperature toughness retention. *J. Build. Eng.* **2025**, *113*, 114050. [\[CrossRef\]](#)

36. Llorca, J. Fatigue of particle-and whisker-reinforced metal-matrix composites. *Prog. Mater. Sci.* **2002**, *47*, 283–353. [\[CrossRef\]](#)

37. Ahmed, U.; Tariq, A.; Nawab, Y.; Shaker, K.; Khaliq, Z.; Umair, M. Comparison of mechanical behavior of biaxial, unidirectional and standard woven fabric reinforced composites. *Fibers Polym.* **2020**, *21*, 1308–1315. [\[CrossRef\]](#)

38. Zhang, Y.; Hu, J.; Dong, S.; Li, Y. Influence of the thickness of pyrolytic carbon interphase on the mechanical behavior of SiC/(BN/PyC)/SiC composites. *Ceram. Int.* **2024**, *50*, 22085–22093. [\[CrossRef\]](#)

39. Liang, C.; Gao, X.; Fu, L.; Mei, H.; Cheng, L.; Zhang, L. Pore evolution and mechanical response under locally varying density defects in ceramic matrix composites. *Compos. Part B Eng.* **2024**, *279*, 111459. [\[CrossRef\]](#)

40. Yan, W.; Fu, Q.; Liang, Y.; Liang, S.; Ai, S. Defect-Induced mechanism analysis and surrogate modeling of tensile strength in woven SiC/SiC composites. *Compos. Part. A Appl. Sci. Manuf.* **2025**, *200*, 109359. [\[CrossRef\]](#)

41. Ren, Z.; Wang, Y.; Ye, Q.; Ye, F.; Kang, R.; Wang, H.; Zhang, X.; Zhang, B.; Zhai, J.; Zhang, J. Tailored Inorganic Fillers in Composite Solid-State Electrolytes: Enabling Synergistic Enhancement of Ionic Conduction and Interfacial Stability for High-Performance ASSLBs. *Small* **2025**, *21*, e08824. [\[CrossRef\]](#)

42. Paksoy, A.H.; Xiao, P. Review of processing and design methodologies of environmental barrier coatings for next generation gas turbine applications. *Adv. Appl. Ceram.* **2023**, *122*, 36–56. [\[CrossRef\]](#)

43. Alnaeli, M.; Alnajideen, M.; Navaratne, R.; Shi, H.; Czyzewski, P.; Wang, P.; Eckart, S.; Alsaegh, A.; Alnasif, A.; Mashruk, S.; et al. High-temperature materials for complex components in ammonia/hydrogen gas turbines: A critical review. *Energies* **2023**, *16*, 6973. [\[CrossRef\]](#)

44. Brown, N.R. Engineering demonstration reactors: A stepping stone on the path to deployment of advanced nuclear energy in the United States. *Energy* **2022**, *238*, 121750. [\[CrossRef\]](#)

45. Carpinteri, A.; Accornero, F. Micro-damage instability mechanisms in composite materials: Cracking coalescence versus fibre ductility and slippage. *Int. J. Damage Mech.* **2025**, *34*, 944–964. [\[CrossRef\]](#)

46. Wang, A.; Ma, Y.; Zhao, D. Pore engineering of porous materials: Effects and applications. *ACS Nano* **2024**, *18*, 22829–22854. [\[CrossRef\]](#) [\[PubMed\]](#)

47. Mostafa, N.H.; Ismarrubie, Z.; Sapuan, S.; Sultan, M. Fibre prestressed polymer-matrix composites: A review. *J. Compos. Mater.* **2017**, *51*, 39–66. [\[CrossRef\]](#)

48. Tang, Z.; Li, A.; Hatakeyama, T.; Shuto, H.; Hayashi, J.-I.; Norinaga, K. Transient three-dimensional simulation of densification process of carbon fibre preforms via chemical vapour infiltration of carbon matrix from methane. *Chem. Eng. Sci.* **2018**, *176*, 107–115. [\[CrossRef\]](#)

49. Zhang, J.; Zhang, Y.; Wang, F.; Li, J.; Li, D.; Liu, R. Long-term oxidation performance of SiCf/SiC composites at 1200 °C in air atmosphere manufactured by PIP and hybrid CVI/PIP techniques. *Ceram. Int.* **2024**, *50*, 10259–10267. [\[CrossRef\]](#)

50. Pandiyarajan, N.; Nunthavarawong, P. Recent advancements in sealants solutions for surface coatings: A comprehensive review. *J. Bio-Tribot-Corros.* **2024**, *10*, 61. [\[CrossRef\]](#)

51. Shrivastava, S.; Rajak, D.K.; Joshi, T.; Singh, D.K.; Mondal, D.P. Ceramic matrix composites: Classifications, manufacturing, properties, and applications. *Ceramics* **2024**, *7*, 652–679. [\[CrossRef\]](#)

52. Polozov, I.; Razumov, N.; Masaylo, D.; Silin, A.; Lebedeva, Y.; Popovich, A. Fabrication of silicon carbide fiber-reinforced silicon carbide matrix composites using binder jetting additive manufacturing from irregularly-shaped and spherical powders. *Materials* **2020**, *13*, 1766. [\[CrossRef\]](#)

53. Panda, H.S.; Sapkal, S.; Panigrahi, S.K. Durability of Structural Adhesive Joints: Factors Affecting Durability, Durability Assessment and Ways to Improve Durability. *Prog. Adhes. Adhes.* **2023**, *7*, 57–111.

54. Reitz, R.B.; Zok, F.W.; Levi, C.G. Reactive alloy melt infiltration for SiC composite matrices: Mechanistic insights. *J. Am. Ceram. Soc.* **2017**, *100*, 5471–5481. [\[CrossRef\]](#)

55. de Jongh, P.E.; Eggenhuisen, T.M. Melt infiltration: An emerging technique for the preparation of novel functional nanostructured materials. *Adv. Mater.* **2013**, *25*, 6672–6690. [\[CrossRef\]](#)

56. Zhong, H.; Wang, Z.; Zhou, H.; Ni, D.; Kan, Y.; Ding, Y.; Dong, S. Properties and microstructure evolution of Cf/SiC composites fabricated by polymer impregnation and pyrolysis (PIP) with liquid polycarbosilane. *Ceram. Int.* **2017**, *43*, 7387–7392. [\[CrossRef\]](#)

57. Pinargote, N.W.S.; Smirnov, A.; Peretyagin, N.; Seleznev, A.; Peretyagin, P. Direct ink writing technology (3D printing) of graphene-based ceramic nanocomposites: A review. *Nanomaterials* **2020**, *10*, 1300. [\[CrossRef\]](#) [\[PubMed\]](#)

58. Kim, I.; Yoon, Y.-J. Digital light processing 3D printing of porous ceramics: A systematic analysis from a debinding perspective. *Addit. Manuf.* **2024**, *93*, 104409. [\[CrossRef\]](#)

59. Maines, E.M.; Porwal, M.K.; Ellison, C.J.; Reineke, T.M. Sustainable advances in SLA/DLP 3D printing materials and processes. *Green Chem.* **2021**, *23*, 6863–6897. [\[CrossRef\]](#)

60. Zhakeyev, A.; Wang, P.; Zhang, L.; Shu, W.; Wang, H.; Xuan, J. Additive manufacturing: Unlocking the evolution of energy materials. *Adv. Sci.* **2017**, *4*, 1700187. [\[CrossRef\]](#)

61. Coltell, M.B.; Lazzeri, A. Chemical vapour infiltration of composites and their applications. In *Chemical Vapour Deposition (CVD)*; CRC Press: Boca Raton, FL, USA, 2019; pp. 363–390.

62. Moradi, S.; Román, F.; Calventus, Y.; Hutchinson, J.M. Densification: A route towards enhanced thermal conductivity of epoxy composites. *Polymers* **2021**, *13*, 286. [\[CrossRef\]](#)

63. Urquiza, E.A.F. Advances in additive manufacturing of polymer-fused deposition modeling on textiles: From 3D printing to innovative 4D printing—A review. *Polymers* **2024**, *16*, 700. [\[CrossRef\]](#)

64. Leng, C.Z.; Losego, M.D. Vapor phase infiltration (VPI) for transforming polymers into organic–inorganic hybrid materials: A critical review of current progress and future challenges. *Mater. Horiz.* **2017**, *4*, 747–771. [\[CrossRef\]](#)

65. Chen, G.; Zeng, Y.; Zhao, F.; Wu, C.; Pan, X.; Lin, F.; Xu, L.; He, Y.; He, G.; Chen, Q.; et al. Conformal fabrication of functional polymer-derived ceramics thin films. *Surf. Coat. Technol.* **2023**, *464*, 129536. [\[CrossRef\]](#)

66. Emonts, C.; Grigat, N.; Merkord, F.; Vollbrecht, B.; Idrissi, A.; Sackmann, J.; Gries, T. Innovation in 3D braiding technology and its applications. *Textiles* **2021**, *1*, 185–205. [\[CrossRef\]](#)

67. Shinde, V.M.; Kamal, A.; Rajasekhar, B.V.; Devasia, R.; Sharma, K. Modeling of industrial isothermal chemical vapor infiltration process for C/SiC structural composites. *J. Am. Ceram. Soc.* **2025**, *108*, e20591. [\[CrossRef\]](#)

68. Daniel, F.; Kucherbaev, P.; Cappiello, C.; Benatallah, B.; Allahbakhsh, M. Quality control in crowdsourcing: A survey of quality attributes, assessment techniques, and assurance actions. *ACM Comput. Surv. (CSUR)* **2018**, *51*, 1–40. [\[CrossRef\]](#)

69. Mohammadkamal, H.; Ajabshir, S.Z.; Mostafaei, A. Additive Manufacturing at the Crossroads: Costs, Sustainability, and Global Adoption. *J. Manuf. Mater. Process.* **2025**, *10*, 5. [\[CrossRef\]](#)

70. Kenarsari, S.D.; Yang, D.; Jiang, G.; Zhang, S.; Wang, J.; Russell, A.G.; Wei, Q.; Fan, M. Review of recent advances in carbon dioxide separation and capture. *RSC Adv.* **2013**, *3*, 22739–22773. [\[CrossRef\]](#)

71. Demiral, M. Strength in adhesion: A multi-mechanics review covering tensile, shear, fracture, fatigue, creep, and impact behavior of polymer bonding in composites. *Polymers* **2025**, *17*, 2600. [\[CrossRef\]](#)

72. Kamalanathan, S. Advanced Damage Detection and Load Optimization in Hybrid Composite Structures Using Multi-Scale Simulation and Machine Learning. *Saudi J. Eng. Technol.* **2025**, *10*, 660–673. [\[CrossRef\]](#)

73. Riaz, Z.; Khan, K.A. Next-Generation Programmable Materials: Multifunctionality, Smart Integration, and Industrial Frontiers. *ES Mater. Manuf.* **2025**, *29*, 1755. [\[CrossRef\]](#)

74. Ionescu, E.; Riedel, R. Polymer processing of ceramics. In *Ceramics and Composites Processing Methods*; Wiley: Hoboken, NJ, USA, 2012; pp. 235–270.

75. Sedeoh, M.M.; Khodadadi, J. Interface behavior and void formation during infiltration of liquids into porous structures. *Int. J. Multiph. Flow* **2013**, *57*, 49–65. [\[CrossRef\]](#)

76. Du, Z.; Song, C.; Guan, K.; Rao, P.; Yang, X.; Bai, L.; Shi, S.; Wang, J.; Liu, Y.; Zeng, Q. Modified C/SiC composites with high ablation resistance: Data-driven intelligent design and experimental validation. *J. Am. Ceram. Soc.* **2025**, *108*, e70209. [\[CrossRef\]](#)

77. Kim, J. Tensile fracture behavior and characterization of ceramic matrix composites. *Materials* **2019**, *12*, 2997. [\[CrossRef\]](#) [\[PubMed\]](#)

78. Zhang, Z.; Li, L.; Chen, Z. Damage evolution and fracture behavior of C/SiC minicomposites with different interphases under uniaxial tensile load. *Materials* **2021**, *14*, 1525. [\[CrossRef\]](#) [\[PubMed\]](#)

79. Yu, M.; Li, H.; Xue, K.; Xie, W.; Zhang, L.; Ren, M.; Fang, L. Effect of microstructure evaluation during the PIP process on macroscopic properties of C/C composites. *Compos. Struct.* **2023**, *308*, 116651. [\[CrossRef\]](#)

80. Valera-Jiménez, J.F.; Marín-Rueda, J.R.; Pérez-Flores, J.C.; Castro-García, M.; Canales-Vázquez, J. Additive manufacturing of functional ceramics. In *3D Printing for Energy Applications*; Wiley: Hoboken, NJ, USA, 2021; pp. 33–67.

81. Yeranee, K.; Rao, Y. A review of recent research on flow and heat transfer analysis in additively manufactured transpiration cooling for gas turbines. *Energies* **2025**, *18*, 3282. [\[CrossRef\]](#)

82. Jldain, H.B. Literature Review on Advanced Textile Reinforcements and Preforms. *Al-Mukhtar J. Eng. Res.* **2021**, *4*, 9–24.

83. Alagha, A.; Singh, S.; Mizouni, R.; Bentahar, J.; Otrok, H. Target localization using multi-agent deep reinforcement learning with proximal policy optimization. *Futur. Gener. Comput. Syst.* **2022**, *136*, 342–357. [\[CrossRef\]](#)

84. Rahman, M.S.U.; Hassan, O.S.; Mustapha, A.A.; Abou-Khousa, M.A.; Cantwell, W.J. Inspection of thick composites: A comparative study between microwaves, X-ray computed tomography and ultrasonic testing. *Nondestruct. Test. Eval.* **2024**, *39*, 2054–2071. [\[CrossRef\]](#)

85. Ortona, A.; Donato, A.; Filacchioni, G.; De Angelis, U.; La Barbera, A.; Nannetti, C.A.; Riccardi, B.; Yeatman, J. SiC–SiCf CMC manufacturing by hybrid CVI–PIP techniques: Process optimisation. *Fusion Eng. Des.* **2000**, *51*, 159–163. [\[CrossRef\]](#)

86. Gleissner, C.; Landsiedel, J.; Bechtold, T.; Pham, T. Surface activation of high performance polymer fibers: A review. *Polym. Rev.* **2022**, *62*, 757–788. [\[CrossRef\]](#)

87. Ilman, M.N.; Muslih, M.R.; Subeki, N.; Wibowo, H. Mitigating distortion and residual stress by static thermal tensioning to improve fatigue crack growth performance of MIG AA5083 welds. *Mater. Des.* **2016**, *99*, 273–283. [\[CrossRef\]](#)

88. Dallaev, R. Advances in materials with self-healing properties: A brief review. *Materials* **2024**, *17*, 2464. [\[CrossRef\]](#) [\[PubMed\]](#)

89. Simões, S. High-performance advanced composites in multifunctional material design: State of the art, challenges, and future directions. *Materials* **2024**, *17*, 5997. [\[CrossRef\]](#) [\[PubMed\]](#)

90. Ramachandran, K.; Bear, J.C.; Jayaseelan, D.D. Oxide-Based Ceramic Matrix Composites for High-Temperature Environments: A Review. *Adv. Eng. Mater.* **2025**, *27*, 2402000. [\[CrossRef\]](#)

91. Bin Rashid, A.; Haque, M.; Islam, S.M.M.; Labib, K.M.R.U.; Chowdhury, P. Breaking boundaries with ceramic matrix composites: A comprehensive overview of materials, manufacturing techniques, transformative applications, recent advancements, and future prospects. *Adv. Mater. Sci. Eng.* **2024**, *2024*, 2112358. [\[CrossRef\]](#)

92. Shvydyuk, K.O.; Nunes-Pereira, J.; Rodrigues, F.F.; Silva, A.P. Review of ceramic composites in aeronautics and aerospace: A multifunctional approach for TPS, TBC and DBD applications. *Ceramics* **2023**, *6*, 195–230. [\[CrossRef\]](#)

93. Agarwal, N.; Rangamani, A.; Bhavsar, K.; Virnodkar, S.S.; Fernandes, A.A.A.; Chadha, U.; Srivastava, D.; Patterson, A.E.; Rajasekharan, V. An overview of carbon–carbon composite materials and their applications. *Front. Mater.* **2024**, *11*, 1374034. [\[CrossRef\]](#)

94. Wyatt, B.C.; Nemani, S.K.; Hilmas, G.E.; Opila, E.J.; Anasori, B. Ultra-high temperature ceramics for extreme environments. *Nat. Rev. Mater.* **2024**, *9*, 773–789. [\[CrossRef\]](#)

95. Guerrero, J.; Mayugo, J.; Costa, J.; Turon, A. A 3D Progressive Failure Model for predicting pseudo-ductility in hybrid unidirectional composite materials under fibre tensile loading. *Compos. Part A Appl. Sci. Manuf.* **2018**, *107*, 579–591. [\[CrossRef\]](#)

96. Chen, X.; Yin, J.; Huang, L.; Lee, S.-H.; Liu, X.; Huang, Z. Microstructural tailoring, mechanical and thermal properties of SiC composites fabricated by selective laser sintering and reactive melt infiltration. *J. Adv. Ceram.* **2023**, *12*, 830–847. [\[CrossRef\]](#)

97. Lin, X.; Salari, M.; Arava, L.M.R.; Ajayan, P.M.; Grinstaff, M.W. High temperature electrical energy storage: Advances, challenges, and frontiers. *Chem. Soc. Rev.* **2016**, *45*, 5848–5887. [\[CrossRef\]](#)

98. Guo, G.; Ye, F.; Cheng, L.; Li, Z.; Zhang, L. A novel porous carbon synthesized to serve in the preparation of highly dense and high-strength SiC/SiC by reactive melt infiltration. *Compos. Part A Appl. Sci. Manuf.* **2024**, *176*, 107839. [\[CrossRef\]](#)

99. Zhang, D.; Zheng, X.; Wang, Z.; Wu, T.; Sohail, A. Effects of braiding architectures on damage resistance and damage tolerance behaviors of 3D braided composites. *Compos. Struct.* **2020**, *232*, 111565. [\[CrossRef\]](#)

100. Zhu, T.; Wang, Z. Advances in processing and ablation properties of carbon fiber reinforced ultra-high temperature ceramic composites. *Rev. Adv. Mater. Sci.* **2024**, *63*, 20240029. [\[CrossRef\]](#)

101. Naslain, R. Design, preparation and properties of non-oxide CMCs for application in engines and nuclear reactors: An overview. *Compos. Sci. Technol.* **2004**, *64*, 155–170. [\[CrossRef\]](#)

102. Zhang, X.-Y.; Fang, G.; Zhou, J. Additively manufactured scaffolds for bone tissue engineering and the prediction of their mechanical behavior: A review. *Materials* **2017**, *10*, 50. [\[CrossRef\]](#)

103. Hatta, H.; Weiss, R.; David, P. Carbon/carbons and their industrial applications. In *Ceramic Matrix Composites: Materials, Modeling and Technology*; Wiley: Hoboken, NJ, USA, 2014; pp. 85–146.

104. Kulik, V.I.; Nilov, A.S.; Bogachev, E.A. High-temperature permanent joints of carbon fiber-reinforced ceramic-matrix composites with similar and other carbonaceous materials. *Refract. Ind. Ceram.* **2022**, *63*, 78–89. [\[CrossRef\]](#)

105. Anwar, W.; Khan, M.Z.; Israr, A.; Mehmood, S.; Anjum, N.A. Effect of structural dynamic characteristics on fatigue and damage tolerance of aerospace grade composite materials. *Aerosp. Sci. Technol.* **2017**, *64*, 39–51. [\[CrossRef\]](#)

106. Barshilia, H.C. Surface modification technologies for aerospace and engineering applications: Current trends, challenges and future prospects. *Trans. Indian Natl. Acad. Eng.* **2021**, *6*, 173–188. [\[CrossRef\]](#)

107. Lee, K.N. Environmental barrier coatings for SiCf/SiC. In *Ceramic Matrix Composites: Materials, Modeling and Technology*; Wiley: Hoboken, NJ, USA, 2014; pp. 430–451.

108. Chen, K.; Seo, D.; Canteenwalla, P. The effect of high-temperature water vapour on degradation and failure of hot section components of gas turbine engines. *Coatings* **2021**, *11*, 1061. [\[CrossRef\]](#)

109. Beaumont, P.W. The structural integrity of composite materials and long-life implementation of composite structures. *Appl. Compos. Mater.* **2020**, *27*, 449–478. [\[CrossRef\]](#)

110. Kurhade, R.R.; Shaikh, M.S.; Nagulwar, V.; Kale, M.A. Advancements in carboxymethyl cellulose (CMC) modifications and their diverse biomedical applications: A comprehensive review. *Int. J. Polym. Mater. Polym. Biomater.* **2025**, *74*, 1043–1067. [\[CrossRef\]](#)

111. Naslain, R.R. SiC–Matrix Composites: Tough Ceramics for Thermostructural Application in Different Fields. In *Engineered Ceramics: Current Status and Future Prospects*; Wiley: Hoboken, NJ, USA, 2016; pp. 142–159.

112. Tuci, G.; Liu, Y.; Rossin, A.; Guo, X.; Pham, C.; Giambastiani, G.; Pham-Huu, C. Porous silicon carbide (SiC): A chance for improving catalysts or just another active-phase carrier? *Chem. Rev.* **2021**, *121*, 10559–10665. [\[CrossRef\]](#) [\[PubMed\]](#)

113. Alagirusamy, R.; Fangueiro, R.; Ogale, V.; Padaki, N. Hybrid yarns and textile preforming for thermoplastic composites. *Text. Prog.* **2006**, *38*, 1–71. [\[CrossRef\]](#)

114. Ghosh, G.; Bhattacharyya, R.; Penumadu, D. Advances in multi-functional composite materials: Applications and opportunities in automotive industry. *Funct. Compos. Struct.* **2025**, *7*, 042001. [\[CrossRef\]](#)

115. Ashofteh, A. Degradation mechanisms and design strategies in environmental barrier coatings: A review. *Int. J. Appl. Ceram. Technol.* **2025**, *23*, e70106. [\[CrossRef\]](#)

116. Yan, S.; Wu, J.; Tan, X.; Deng, Z.; Mao, J.; Jia, L.; Liu, M.; Chen, H.; Jiang, L.; Zhang, X. Microstructural evolution and corrosion mechanism of thermal/environmental barrier coatings against molten calcium–magnesium–alumino–silicate. *Surf. Coat. Technol.* **2024**, *478*, 130433. [\[CrossRef\]](#)

117. Lee, K.N.; Zhu, D.; Lima, R.S. Perspectives on environmental barrier coatings (EBCs) manufactured via air plasma spray (APS) on ceramic matrix composites (CMCs): A tutorial paper. *J. Therm. Spray Technol.* **2021**, *30*, 40–58. [\[CrossRef\]](#)

118. Tavares, S.M.O.; Ribeiro, J.A.; Ribeiro, B.A.; de Castro, P.M.S.T. Aircraft structural design and life-cycle assessment through digital twins. *Designs* **2024**, *8*, 29. [\[CrossRef\]](#)

119. Zhang, L.; Lin, H.; Sun, Z.; Cai, X.; Feng, T.; Wen, Z.; Sun, S. Investigation of in-situ microstructural mechanical properties and thermal damage mechanisms of SiCf/SiC under CVI and PIP processes. *Mater. Charact.* **2025**, *220*, 114689. [\[CrossRef\]](#)

120. Gavalda-Diaz, O.; Saiz, E.; Chevalier, J.; Bouville, F. Toughening of ceramics and ceramic composites through microstructure engineering: A review. *Int. Mater. Rev.* **2025**, *70*, 3–30. [\[CrossRef\]](#)

121. Morscher, G.N. Tensile creep and rupture of 2D-woven SiC/SiC composites for high temperature applications. *J. Eur. Ceram. Soc.* **2010**, *30*, 2209–2221. [\[CrossRef\]](#)

122. Patel, A.; Sato, E.; Takagi, T.; Shichijo, N. Effect of oxidation on the bending fatigue behavior of an advanced SiC/SiC CMC component at 1000 °C in air. *J. Eur. Ceram. Soc.* **2022**, *42*, 4121–4132. [\[CrossRef\]](#)

123. Wang, Y.; Ma, Y.; Chen, Y.; Ding, B. Exploring the toughening mechanisms of PyC interphase in SiCf/SiC composites through molecular dynamics and mesoscale stochastic simulations. *Eng. Fract. Mech.* **2024**, *310*, 110445. [\[CrossRef\]](#)

124. Prasad, N.E.; Bhaduri, S.B. Monolithic Ceramics for Aerospace Applications. In *Aerospace Materials and Material Technologies: Volume 1: Aerospace Materials*; Springer: Singapore, 2016; pp. 415–437.

125. Kulkarni, A.; James, A.; Kamel, A. Advanced materials and manufacturing technology developments for extreme environment gas turbine applications. *Mater. Perform. Charact.* **2021**, *10*, 146–160. [\[CrossRef\]](#)

126. Ding, Z.; Pan, J.; Peng, L.; Zhang, H.; Hu, B.; Li, J.; Luo, A.A. The effect of microstructure on the plastic strain localization and fatigue crack initiation in cast Mg–8Gd–3Y–0.5 Zr alloy. *Mater. Sci. Eng. A* **2021**, *801*, 140383. [\[CrossRef\]](#)

127. Grujicic, M.; Snipes, J.S.; Galgalikar, R.; Yavari, R.; Avuthu, V.; Ramaswami, S. Multi-length-scale derivation of the room-temperature material constitutive model for SiC/SiC ceramic-matrix composites. *Proc. Inst. Mech. Eng. Part L J. Mater. Des. Appl.* **2017**, *231*, 443–462. [\[CrossRef\]](#)

128. Yin, X.W.; Cheng, L.F.; Zhang, L.T.; Travitzky, N.; Greil, P. Fibre-reinforced multifunctional SiC matrix composite materials. *Int. Mater. Rev.* **2017**, *62*, 117–172. [\[CrossRef\]](#)

129. Chi, Y.; Li, M.; Xu, L.; Sun, Q. Phase transition induced interfacial debonding in shape memory alloy fiber–matrix system. *Int. J. Solids Struct.* **2015**, *75*, 199–210. [\[CrossRef\]](#)

130. Lei, Z.; Ma, J.; Luo, G.; Li, Q.; Sun, W.; Yin, B. Mechanical Performance and Electrical Resistance Properties of Plain Woven Carbon Fiber-Reinforced Epoxy Composites under Quasi-Static and Cyclic Loading. *Polym. Compos.* **2025**, *1*–15. [\[CrossRef\]](#)

131. Miao, C.; Zhiwei, C.; Qiaoyi, X.; Bolin, T.; Wen, W.; Zhengwei, D.; Jie, Y.; Mingling, W. Anisotropic Thermal Expansion Behaviors and Damage Evolution Mechanisms of 3D Angle-Interlocked Woven Composites Subjected to Thermal Cycling. *Polym. Compos.* **2025**, *47*, 1661–1675. [\[CrossRef\]](#)

132. Lei, Z.; Liu, Y.; Ma, F.; Song, Z.; Li, Y. Oxidation resistance of TiAlN/ZrN multilayer coatings. *Vacuum* **2016**, *127*, 22–29. [\[CrossRef\]](#)

133. Olsson, R. A survey of test methods for multiaxial and out-of-plane strength of composite laminates. *Compos. Sci. Technol.* **2011**, *71*, 773–783. [\[CrossRef\]](#)

134. Volkmann, E.; Tushtev, K.; Koch, D.; Wilhelmi, C.; Göring, J.; Rezwan, K. Assessment of three oxide/oxide ceramic matrix composites: Mechanical performance and effects of heat treatments. *Compos. Part A Appl. Sci. Manuf.* **2015**, *68*, 19–28. [\[CrossRef\]](#)

135. Xu, Y.; Hu, X.; Xu, F.; Li, K. Rare earth silicate environmental barrier coatings: Present status and prospective. *Ceram. Int.* **2017**, *43*, 5847–5855. [\[CrossRef\]](#)

136. Paladugu, S.R.M.; Sreekanth, P.S.R.; Sahu, S.K.; Naresh, K.; Karthick, S.A.; Venkateshwaran, N.; Ramoni, M.; Mensah, R.A.; Das, O.; Shanmugam, R. A comprehensive review of self-healing polymer, metal, and ceramic matrix composites and their modeling aspects for aerospace applications. *Materials* **2022**, *15*, 8521. [\[CrossRef\]](#)

137. Mahmood, A.; Perveen, F.; Chen, S.; Akram, T.; Irfan, A. Polymer composites in 3D/4D printing: Materials, advances, and prospects. *Molecules* **2024**, *29*, 319. [\[CrossRef\]](#)

138. Naslain, R.R. Processing of non-oxide ceramic matrix composites: An overview. *Adv. Sci. Technol.* **2006**, *50*, 64–74. [\[CrossRef\]](#)

139. Evans, A.G.; Clarke, D.R.; Levi, C.G. The influence of oxides on the performance of advanced gas turbines. *J. Eur. Ceram. Soc.* **2008**, *28*, 1405–1419. [\[CrossRef\]](#)

140. Gautam, D.; Gautam, Y.K. Applications of thermal spray-based coatings for renewable energy. In *Multifunctional Nanostructured Coatings*; Woodhead Publishing: Cambridge, UK, 2025; pp. 457–478.

141. Darolia, R. Development of strong, oxidation and corrosion resistant nickel-based superalloys: Critical review of challenges, progress and prospects. *Int. Mater. Rev.* **2019**, *64*, 355–380. [\[CrossRef\]](#)

142. Grant, K.M.; Krämer, S.; Löfvander, J.P.; Levi, C.G. CMAS degradation of environmental barrier coatings. *Surf. Coat. Technol.* **2007**, *202*, 653–657. [\[CrossRef\]](#)

143. Wang, Z.; Muránsky, O.; Zhu, H.; Wei, T.; Zhang, Z.; Ionescu, M.; Yang, C.; Davis, J.; Hu, G.; Munroe, P.; et al. Impact of pre-existing crystal lattice defects on the accumulation of irradiation-induced damage in a C/C composite. *J. Nucl. Mater.* **2022**, *564*, 153684. [\[CrossRef\]](#)

144. Ouyang, J.-H.; Cao, G.; Wang, S.-Q. Environmental Barrier Coatings (EBCs) for Silicon-Based Ceramics and Composites. In *Ceramic Coatings for High-Temperature Environments: From Thermal Barrier to Environmental Barrier Applications*; Springer International Publishing: Cham, Switzerland, 2023; pp. 243–281.

145. Handschuh-Wang, S.; Wang, T.; Gancarz, T.; Liu, X.; Wang, B.; He, B.; Dickey, M.D.; Wimmer, G.W.; Stadler, F.J. The liquid metal age: A transition from Hg to Ga. *Adv. Mater.* **2024**, *36*, e2408466. [\[CrossRef\]](#) [\[PubMed\]](#)

146. Perepezko, J. High temperature environmental resistant Mo-Si-B based coatings. *Int. J. Refract. Met. Hard Mater.* **2018**, *71*, 246–254. [\[CrossRef\]](#)

147. Piascik, B.; Vickers, J.; Lowry, D.; Scotti, S.; Stewart, J.; Calomino, A. *Materials, Structures, Mechanical Systems, and Manufacturing Roadmap*; NASA: Washington, DC, USA, 2012; pp. 12–22.

148. Webster, C.S. Safety in unpredictable complex systems—a framework for the analysis of safety derived from the nuclear power industry. *Prometheus* **2016**, *34*, 115–132. [\[CrossRef\]](#)

149. Spray, U.T. *Review of Progress in Quantitative Nondestructive Evaluation: Volume 16*; Springer Science & Business Media: Berlin/Heidelberg, Germany, 1998; Volume 7, p. 9.

150. Farahmand, B. Ceramic Matrix Composites (CMCs) (Methods of Manufacturing CMC Parts). In *Fundamentals of Composites and Their Methods of Fabrications: PMCs, MMCs, and CMCs*; Springer Nature: Cham, Switzerland, 2025; pp. 129–159.

151. Chen, D.; Pegler, A.; Dwivedi, G.; De Wet, D.; Dorfman, M. Thermal cycling behavior of air plasma-sprayed and low-pressure plasma-sprayed environmental barrier coatings. *Coatings* **2021**, *11*, 868. [\[CrossRef\]](#)

152. Yavuz, M.T.; Ozkol, I. Thermal Structural Design Aspects of Military Aircraft. *J. Aeronaut. Space Technol. Hava. Ve Uzay Teknol. Derg.* **2024**, *17*, 124–158.

153. Süß, F.; Schöffler, R.; Friedrich, L.; Petersen, A.; Vogel, F.; Frieß, M.; Ebach-Stahl, A. Design and Manufacture of SiC/SiC Nozzle Guide Vanes with Environmental Barrier Coatings for High-Pressure Turbines. *J. Eng. Gas Turbines Power* **2025**, *147*, 021021. [\[CrossRef\]](#)

154. Papenburg, U.; Walter, S.; Selzer, M.; Beyer, S.; Laube, H.; Langel, G. Advanced ceramic matrix composites (CMC's) for space propulsion systems. In Proceedings of the 33rd Joint Propulsion Conference and Exhibit, Seattle, WA, USA, 6–9 July 1997; p. 3391.

155. Jurf, R.A.; Butner, S.C. Advances in oxide-oxide CMC. *J. Eng. Gas Turbines Power* **2000**, *122*, 202–205. [\[CrossRef\]](#)

156. Nair, R.B.; Brabazon, D. Calcia magnesia alumino silicate (CMAS) corrosion attack on thermally sprayed thermal barrier coatings: A comprehensive review. *npj Mater. Degrav.* **2024**, *8*, 44. [\[CrossRef\]](#)

157. Wang, W.; Zhao, D.; Zheng, B.; Wang, S.; Zeng, B.; Zhu, Z.; Ye, H. Current research advances in high-overload-resistant multimode strapdown optoelectronic systems. In Proceedings of the Second Conference of Young Scientists of the Chinese Society of Optical Engineering, Ningbo, China, 25–27 April 2025; Volume 13799, pp. 831–850.

158. Simos, N.; Quaranta, E.; Charitonidis, N.; Sprouster, D.; Zhong, Z.; Ghose, S.; Kotsina, Z.; Assmann, R.; Redaelli, S.; Bertarelli, A.; et al. Radiation damage of a two-dimensional carbon fiber composite (CFC). *Carbon Trends* **2021**, *3*, 100028. [\[CrossRef\]](#)

159. Koyanagi, T.; Katoh, Y.; Nozawa, T.; Snead, L.L.; Kondo, S.; Henager, C.H., Jr.; Ferraris, M.; Hinoki, T.; Huang, Q. Recent progress in the development of SiC composites for nuclear fusion applications. *J. Nucl. Mater.* **2018**, *511*, 544–555. [\[CrossRef\]](#)

160. Lu, Y.; Cao, Y.; Zhao, X. Optimal rare-earth disilicates as top coat in multilayer environmental barrier coatings. *J. Alloy. Compd.* **2018**, *769*, 1026–1033. [\[CrossRef\]](#)

161. Chen, M.; Fang, G.; Gao, X.; Song, Y. Thermo-Mechanical Stress Distributions in a Ceramic Matrix Composites Turbine Vane Coated with Environmental Barrier Coatings. *Coatings* **2024**, *14*, 87. [\[CrossRef\]](#)

162. Kumar, M.H.; Moganapriya, C.; Kumar, A.M.; Rajasekar, R.; Gobinath, V.K. Self-Healing Materials in Aerospace Applications. In *Self-Healing Smart Materials and Allied Applications*; Wiley: Hoboken, NJ, USA, 2021; pp. 415–434.

163. Chen, X.; Li, J.; Deng, T.; Meng, S.; Wang, G. Mechanisms of the Ti-enhanced ablation resistance in a Zr-Si-BC ceramic achieving the reduced ablation rate and long-term durability. *Aerosp. Sci. Technol.* **2025**, *168*, 110973. [\[CrossRef\]](#)

164. Guo, Y.; Bai, B.; Zhao, S.; Guo, L.; Guo, H. Laser-induced triple-scale microstructure enables strain-tolerant (Gd0. 9Yb0. 1) 2Zr2O7/YSZ coatings with decoupled CMAS/thermal shock degradation. *J. Eur. Ceram. Soc.* **2025**, *46*, 117971. [\[CrossRef\]](#)

165. Monceau, D.; Vilasi, M. High temperature oxidation of additively manufactured structural alloys. *JOM* **2022**, *74*, 1659–1667. [\[CrossRef\]](#)

166. Pham, H.V.; Kurata, M.; Steinbrueck, M. Steam oxidation of silicon carbide at high temperatures for the application as accident tolerant fuel cladding, an overview. *Thermo* **2021**, *1*, 151–167. [\[CrossRef\]](#)

167. Wang, C.; Liu, M.; Feng, J.; Zhang, X.; Deng, C.; Zhou, K.; Zeng, D.; Guo, S.; Zhao, R.; Li, S. Water vapor corrosion behavior of Yb_2SiO_5 environmental barrier coatings prepared by plasma spray-physical vapor deposition. *Coatings* **2020**, *10*, 392. [\[CrossRef\]](#)

168. Iqbal, A.; Moskal, G. Recent development in advance ceramic materials and understanding the mechanisms of thermal barrier coatings degradation. *Arch. Comput. Methods Eng.* **2023**, *30*, 4855–4896. [\[CrossRef\]](#)

169. Xiao, Y.; Yang, L.; Zhu, W.; Zhou, Y.; Pi, Z.; Wei, Y. Delamination mechanism of thermal barrier coatings induced by thermal cycling and growth stresses. *Eng. Fail. Anal.* **2021**, *121*, 105202. [\[CrossRef\]](#)

170. Dada, M.; Popoola, P. Recent advances in joining technologies of aluminum alloys: A review. *Discov. Mater.* **2024**, *4*, 86. [\[CrossRef\]](#)

171. Gan, Y.X. Effect of interface structure on mechanical properties of advanced composite materials. *Int. J. Mol. Sci.* **2009**, *10*, 5115–5134. [\[CrossRef\]](#) [\[PubMed\]](#)

172. Sobczak, N.; Sobczak, J.; Asthana, R.; Purgert, R. The mystery of molten metal. *China Foundry* **2010**, *7*, 425–437.

173. Gunwant, D. Interfacial strengthening in bio-inspired materials: A review. *Compos. Interfaces* **2025**, *32*, 509–585. [\[CrossRef\]](#)

174. Shinde, S.V.; Sampath, S. Interplay between cracking and delamination in incrementally deposited plasma sprayed coatings. *Acta Mater.* **2021**, *215*, 117074. [\[CrossRef\]](#)

175. Lazzeri, A. CVI processing of ceramic matrix composites. In *Ceramics and Composites Processing Methods*; Wiley: Hoboken, NJ, USA, 2012; pp. 313–349.

176. Poerschke, D.; Van Sluytman, J.; Wong, K.; Levi, C. Thermochemical compatibility of ytterbia–(hafnia/silica) multilayers for environmental barrier coatings. *Acta Mater.* **2013**, *61*, 6743–6755. [\[CrossRef\]](#)

177. Kane, K.; Garcia, E.; Stack, P.; Lance, M.; Parker, C.; Sampath, S.; Pint, B.A. Evaluating steam oxidation kinetics of environmental barrier coatings. *J. Am. Ceram. Soc.* **2022**, *105*, 590–605. [\[CrossRef\]](#)

178. Shah, S.R.; Raj, R. Multilayer design and evaluation of a high temperature environmental barrier coating for Si-based ceramics. *J. Am. Ceram. Soc.* **2007**, *90*, 516–522. [\[CrossRef\]](#)

179. Mujtaba, M.; Lippinen, J.; Ojanen, M.; Puttonen, S.; Vaittinen, H. Trends and challenges in the development of bio-based barrier coating materials for paper/cardboard food packaging; a review. *Sci. Total. Environ.* **2022**, *851*, 158328. [\[CrossRef\]](#)

180. Richards, B.T.; Sehr, S.; de Franqueville, F.; Begley, M.R.; Wadley, H.N. Fracture mechanisms of ytterbium monosilicate environmental barrier coatings during cyclic thermal exposure. *Acta Mater.* **2016**, *103*, 448–460. [\[CrossRef\]](#)

181. Padture, N.P.; Gell, M.; Jordan, E.H. Thermal barrier coatings for gas-turbine engine applications. *Science* **2002**, *296*, 280–284. [\[CrossRef\]](#) [\[PubMed\]](#)

182. Murty, S.V.S.N.; Sharma, S.C. Materials for Indian space program: An overview. *J. Indian Inst. Sci.* **2022**, *102*, 513–559. [\[CrossRef\]](#)

183. Katoh, Y.; Snead, L.L.; Szlufarska, I.; Weber, W.J. Radiation effects in SiC for nuclear structural applications. *Curr. Opin. Solid State Mater. Sci.* **2012**, *16*, 143–152. [\[CrossRef\]](#)

184. Pasquali, M.; Bertarelli, A.; Accettura, C.; Berthome, E.; Bianchi, L.; Bolz, P.; Carra, F.; Fichera, C.; Frankl, M.I.; Furness, T.; et al. Dynamic response of advanced materials impacted by particle beams: The MultiMat experiment. *J. Dyn. Behav. Mater.* **2019**, *5*, 266–295. [\[CrossRef\]](#)

185. Yaramasu, V.; Wu, B.; Sen, P.C.; Kouro, S.; Narimani, M. High-power wind energy conversion systems: State-of-the-art and emerging technologies. *Proc. IEEE* **2015**, *103*, 740–788. [\[CrossRef\]](#)

186. Kumar, K.; Kumar, S.; Gill, H.S. Role of Carbide-Based Thermal-Sprayed Coatings to Prevent Failure for Boiler Steels: A Review. *J. Fail. Anal. Prev.* **2024**, *24*, 1628–1663. [\[CrossRef\]](#)

187. Yu, W.; Liu, C.; Qiu, L.; Zhang, P.; Ma, W.; Yue, Y.; Xie, H.; Larkin, L.S. Advanced thermal interface materials for thermal management. *Eng. Sci.* **2018**, *2*, 1–3. [\[CrossRef\]](#)

188. da Silva, C.M.I.; Cabrita, C.M.P.; Matias, J.C.d.O. Proactive reliability maintenance: A case study concerning maintenance service costs. *J. Qual. Maint. Eng.* **2008**, *14*, 343–355. [\[CrossRef\]](#)

189. Singh, J.; Gill, H.S. Evolution of nickel-based superalloy claddings for against high-temperature oxidation and wear. In *Thermal Claddings for Engineering Applications*; CRC Press: Boca Raton, FL, USA, 2024; pp. 160–181.

190. Shrestha, S.; Francis, R.; Smith, A. Alloy selection for wear-resistant lightweight aluminium brake disc. *Surf. Eng.* **2024**, *40*, 142–156. [\[CrossRef\]](#)

191. Xu, C.; Jia, C.; Peng, Z.; Chen, S. High-temperature properties and microstructure evolution of C/C-ZrC-SiC composites fabricated by reactive melt infiltration. *J. Eur. Ceram. Soc.* **2025**, *45*, 117288. [\[CrossRef\]](#)

192. Hanninen, H.; Aaltonen, P.; Brederholm, A.; Ehrnsten, U.; Gripenberg, H.; Toivonen, A.; Pitkanen, J.; Virkkunen, I. Dissimilar metal weld joints and their performance in nuclear power plant and oil refinery conditions. *Vtt Tied.* **2006**, *2347*, 208.

193. Tang, S.; Deng, J.; Wang, S.; Liu, W.; Yang, K. Ablation behaviors of ultra-high temperature ceramic composites. *Mater. Sci. Eng. A* **2007**, *465*, 1–7. [\[CrossRef\]](#)

194. Zheng, L.; Ambrosetti, M.; Tronconi, E. Joule-heated catalytic reactors toward decarbonization and process intensification: A review. *ACS Eng. Au* **2023**, *4*, 4–21. [\[CrossRef\]](#)

195. Noor, A.K.; Veneri, S.L. Perspectives on future aeronautical and space systems. *Prog. Astronaut. Aeronaut.* **1997**, *172*, 1–40.

196. Vijay, V.V. Exploring the Frontiers: A Comprehensive Review on Modified Polycarbosilanes as Precursors for Advanced Inorganic Materials. *Polym. Rev.* **2025**, *65*, 329–364. [\[CrossRef\]](#)

197. Beshchasna, N.; Saqib, M.; Kraskiewicz, H.; Wasyluk, Ł.; Kuzmin, O.; Duta, O.C.; Ficai, D.; Ghizdavet, Z.; Marin, A.; Ficai, A.; et al. Recent advances in manufacturing innovative stents. *Pharmaceutics* **2020**, *12*, 349. [\[CrossRef\]](#)

198. Lin, H.; Becher, P.F. High-Temperature Creep Deformation of Alumina–SiC-Whisker Composites. *J. Am. Ceram. Soc.* **1991**, *74*, 1886–1893. [\[CrossRef\]](#)

199. Nieto, A.; Agrawal, R.; Bravo, L.; Hofmeister-Mock, C.; Pepi, M.; Ghoshal, A. Calcia–magnesia–alumina–silicate (CMAS) attack mechanisms and roadmap towards Sandphobic thermal and environmental barrier coatings. *Int. Mater. Rev.* **2021**, *66*, 451–492. [\[CrossRef\]](#)

200. Wali, N.; Yang, J. Reactive Melt-Infiltration Processing of Fiber-Reinforced Ceramic Matrix Composites. In *Ceramics and Composites Processing Methods*; Wiley: Hoboken, NJ, USA, 2012; pp. 351–390.

201. Yu, Y.; Liu, X.; Yan, J.; Wang, Y.; Qing, X. Real-time life-cycle monitoring of composite structures using piezoelectric-fiber hybrid sensor network. *Sensors* **2021**, *21*, 8213. [\[CrossRef\]](#)

202. Bose, S.; Akdogan, E.K.; Balla, V.K.; Ciliveri, S.; Colombo, P.; Franchin, G.; Ku, N.; Kushram, P.; Niu, F.; Pelz, J.; et al. 3D printing of ceramics: Advantages, challenges, applications, and perspectives. *J. Am. Ceram. Soc.* **2024**, *107*, 7879–7920. [\[CrossRef\]](#)

203. Sanchez, V.; Walsh, C.J.; Wood, R.J. Textile technology for soft robotic and autonomous garments. *Adv. Funct. Mater.* **2021**, *31*, 2008278. [\[CrossRef\]](#)

204. Saadi, M.A.S.R.; Maguire, A.; Pottackal, N.T.; Thakur, S.H.; Ikram, M.M.; Hart, A.J.; Ajayan, P.M.; Rahman, M.M. Direct ink writing: A 3D printing technology for diverse materials. *Adv. Mater.* **2022**, *34*, e2108855. [\[CrossRef\]](#) [\[PubMed\]](#)

205. Martinez-Val, R.; Perez, E. Aeronautics and astronautics: Recent progress and future trends. *Proc. Inst. Mech. Eng. Part C J. Mech. Eng. Sci.* **2009**, *223*, 2767–2820. [\[CrossRef\]](#)

206. Ning, Y.; Liu, F.; Ran, L.; Peng, K.; Ge, Y.; Yi, M. Effect of preparation method on the mechanism for oxidation of C/C-BN composites. *Ceram. Int.* **2022**, *48*, 525–539. [\[CrossRef\]](#)

207. Eswarappa Prameela, S.; Pollock, T.M.; Raabe, D.; Meyers, M.A.; Aitkaliyeva, A.; Chintersingh, K.L.; Cordero, Z.C.; Graham-Brady, L. Materials for extreme environments. *Nat. Rev. Mater.* **2023**, *8*, 81–88. [\[CrossRef\]](#)

208. Han, P.; Wang, Q.; Niu, W.; Li, N.; Qian, R.; Wan, M. Multi-layer formation by oxidation and solid-state crystallization of cold sprayed amorphous coatings during dry sliding wear. *Wear* **2024**, *558*, 205553. [\[CrossRef\]](#)

209. Thakur, A.; Kumar, A. Self-healing ceramic coatings. In *Advanced Ceramic Coatings for Emerging Applications*; Elsevier: Amsterdam, The Netherlands, 2023; pp. 19–42.

210. Fernandez, C.A.; Correa, M.; Nguyen, M.-T.; Rod, K.A.; Dai, G.L.; Cosimescu, L.; Rousseau, R.; Glezakou, V.-A. Progress and challenges in self-healing cementitious materials. *J. Mater. Sci.* **2021**, *56*, 201–230. [\[CrossRef\]](#)

211. Piquero, T.; Vincent, H.; Vincent, C.; Bouix, J. Influence of carbide coatings on the oxidation behavior of carbon fibers. *Carbon* **1995**, *33*, 455–467. [\[CrossRef\]](#)

212. Chai, Q.; Luo, Y.; Ren, J.; Zhang, J.; Yang, J.; Yuan, L.; Peng, G.D. Review on fiber-optic sensing in health monitoring of power grids. *Opt. Eng.* **2019**, *58*, 072007. [\[CrossRef\]](#)

213. Travitzky, N.; Bonet, A.; Dermeik, B.; Fey, T.; Filbert-Demut, I.; Schlier, L.; Schlöldt, T.; Greil, P. Additive manufacturing of ceramic-based materials. *Adv. Eng. Mater.* **2014**, *16*, 729–754. [\[CrossRef\]](#)

214. Lim, D.D.; Parashivamurthy, V.; Lee, J.-H.; Zhao, X.; Kaul, A.; Gheytani, S.; Gu, G.X. Enhancing the fracture resistance of 3D printed Zirconia via gyroid structures. *Scr. Mater.* **2025**, *268*, 116888. [\[CrossRef\]](#)

215. Dede, E.M.; Zhou, F.; Zhou, Y.; Lohan, D.J.; Asheghi, M.; Goodson, K.E.; Erickson, K. Applications, Design Methods, and Challenges for Additive Manufacturing of Thermal Solutions for Heterogeneous Integration of Electronics. *J. Electron. Packag.* **2025**, *147*, 021009. [\[CrossRef\]](#)

216. Jindal, H.; Kaur, S. Robotics and automation in textile industry. *Int. J. Sci. Res. Sci. Eng. Technol.* **2021**, *8*, 40–45. [\[CrossRef\]](#)

217. Rahman, S.; Hasan, S.; Nitai, A.S.; Nam, S.; Karmakar, A.K.; Ahsan, S.; Shiddiky, M.J.A.; Ahmed, M.B. Recent developments of carboxymethyl cellulose. *Polymers* **2021**, *13*, 1345. [\[CrossRef\]](#)

218. Anisetti, M.; Ardagna, C.; Damiani, E.; El Ioini, N.; Gaudenzi, F. Modeling time, probability, and configuration constraints for continuous cloud service certification. *Comput. Secur.* **2018**, *72*, 234–254. [\[CrossRef\]](#)

219. Takeishi, K.; Krewinkel, R. Advanced gas turbine cooling for the carbon-neutral era. *Int. J. Turbomach. Propuls. Power* **2023**, *8*, 19. [\[CrossRef\]](#)

220. Bathias, C. An engineering point of view about fatigue of polymer matrix composite materials. *Int. J. Fatigue* **2006**, *28*, 1094–1099. [\[CrossRef\]](#)

221. Xu, X.; Luan, X.; Lv, S.; Yang, X.; Chen, X.; Cheng, L.; Riedel, R. Long-term oxidation resistant SiC/SiC-SiHfBCN composites: A promising thermo-structural material aims for hypersonic roundtrip. *Ceram. Int.* **2023**, *49*, 38803–38812. [\[CrossRef\]](#)

222. Park, M.-S.; Gu, J.; Lee, H.; Lee, S.-H.; Feng, L.; Fahrenholz, W.G. Cf/SiC ceramic matrix composites with extraordinary thermomechanical properties up to 2000° C. *Nanomaterials* **2023**, *14*, 72. [\[CrossRef\]](#)

223. Wang, X.; Gao, X.; Zhang, Z.; Cheng, L.; Ma, H.; Yang, W. Advances in modifications and high-temperature applications of silicon carbide ceramic matrix composites in aerospace: A focused review. *J. Eur. Ceram. Soc.* **2021**, *41*, 4671–4688. [\[CrossRef\]](#)

224. Qian, B.; Wang, Y.; Zu, J.; Xu, K.; Shang, Q.; Bai, Y. A review on multicomponent rare earth silicate environmental barrier coatings. *J. Mater. Res. Technol.* **2024**, *29*, 1231–1243. [\[CrossRef\]](#)

225. Liu, Z.; Li, Z.; Li, Q.; Wang, C.; Chen, P.; Yang, L.; Zhang, L.; Su, B.; Yan, C.; Shi, Y. Ultra-High strength and toughness continuous SiCf/SiC ceramic matrix composites prepared by an additive manufacturing manipulator. *J. Eur. Ceram. Soc.* **2025**, *45*, 117176. [\[CrossRef\]](#)

226. Alexander, M.; Beushausen, H. Durability, service life prediction, and modelling for reinforced concrete structures—review and critique. *Cem. Concr. Res.* **2019**, *122*, 17–29. [\[CrossRef\]](#)

227. Yuan, L.; Chenglong, W.; Yongchao, S.; Mingbo, S.; Yu, Y.; Zhan, G.; Yiwen, X. Review on creep phenomenon and its model in aircraft engines. *Int. J. Aerosp. Eng.* **2023**, *2023*, 4465565. [\[CrossRef\]](#)

228. Kumar, M.; Devi, C.; Hemath, M.; Mandol, S.; Rangappa, S.M.; Siengchin, S. Prospects of ceramic matrix composites in engineering and commercial applications. In *Applications of Composite Materials in Engineering*; Woodhead Publishing: Cambridge, UK, 2025; pp. 419–436. [[CrossRef](#)]

229. Al-Momani, H.; Al Meanazel, O.T.; Kwaldeh, E.; Alaween, A.; Khasaleh, A.; Qamar, A. The efficiency of using a tailored inventory management system in the military aviation industry. *Helijon* **2020**, *6*, e04424. [[CrossRef](#)]

230. Marimuthu, R.; Sankaranarayanan, B. Optimizing sustainable manufacturing: A comprehensive analysis of innovative technologies and strategic interventions. In *Green Manufacturing*; CRC Press: Boca Raton, FL, USA; pp. 216–240. [[CrossRef](#)]

231. Han, Z.; Zhou, J.; Lu, G.; Piao, Z.; Tao, S.; Gao, R.; Li, C.; Zhang, X.; Zhou, G. Uncovering battery electrochemical mechanisms by artificial intelligence. *Natl. Sci. Rev.* **2025**, *12*, nwaf442. [[CrossRef](#)]

232. Singh, V.; Patra, S.; Murugan, N.A.; Toncu, D.-C.; Tiwari, A. Recent trends in computational tools and data-driven modeling for advanced materials. *Mater. Adv.* **2022**, *3*, 4069–4087. [[CrossRef](#)]

233. Fernie, J.A.; Drew, R.A.L.; Knowles, K.M. Joining of engineering ceramics. *Int. Mater. Rev.* **2009**, *54*, 283–331. [[CrossRef](#)]

234. Zhou, Y.; Gong, D.-C.; Huang, B.; Peters, B.A. The impacts of carbon tariff on green supply chain design. *IEEE Trans. Autom. Sci. Eng.* **2015**, *14*, 1542–1555. [[CrossRef](#)]

Disclaimer/Publisher’s Note: The statements, opinions and data contained in all publications are solely those of the individual author(s) and contributor(s) and not of MDPI and/or the editor(s). MDPI and/or the editor(s) disclaim responsibility for any injury to people or property resulting from any ideas, methods, instructions or products referred to in the content.